R&D Needs for Reduced Order H_2 Release/Ignition Behavior Models – The SNL Perspective

Isaac Ekoto
Principle Investigator

Daniel Dedrick
Hydrogen Program Manager

Bill Houf (retired), Terry Johnson, Adam Ruggles, Aaron Harris
Sandia National Laboratories

Antonio Ruiz
Program Manager:
DOE FCT Codes and Standards Program Element

October 17, 2012

Sandia is a multi-program laboratory operated by Sandia Corporation, a Lockheed Martin Company, for the United States Department of Energy under contract DE-AC04-94AL85000

Alt. Title…

How best can risk management approaches incorporate H_2 behavior models?

One first needs to decide the appropriate risk approach: Prescriptive vs. QRA

Example: Pipe rupture potential from internal pressure

- Reference extreme pressure selected (e.g., MAWP)
- Validated method used to compute hoop stresses
- Safety Factor (SF) used to account for QAQC issues and uncertainty in calculation methods

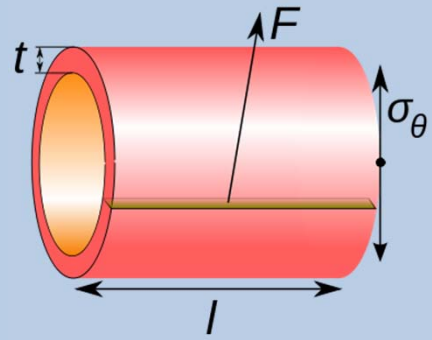

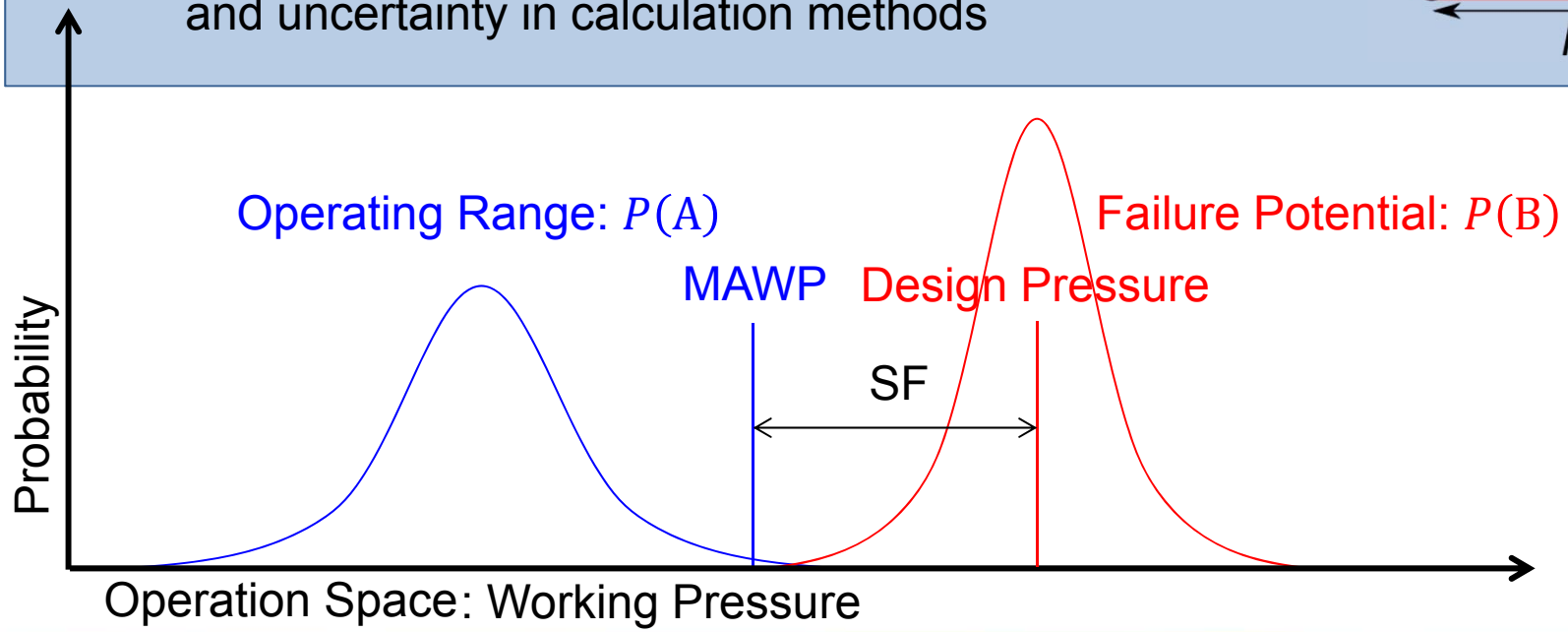

How best can risk management approaches incorporate H_2 behavior models?

QRA

Example: Pipe rupture potential from internal pressure

- Risk calculated from overlapping operation and failure probabilities
- Acceptance criteria based on integrated risk potential
- Cumulative system risk considered: $Risk_{System} = \sum_i Risk_i$

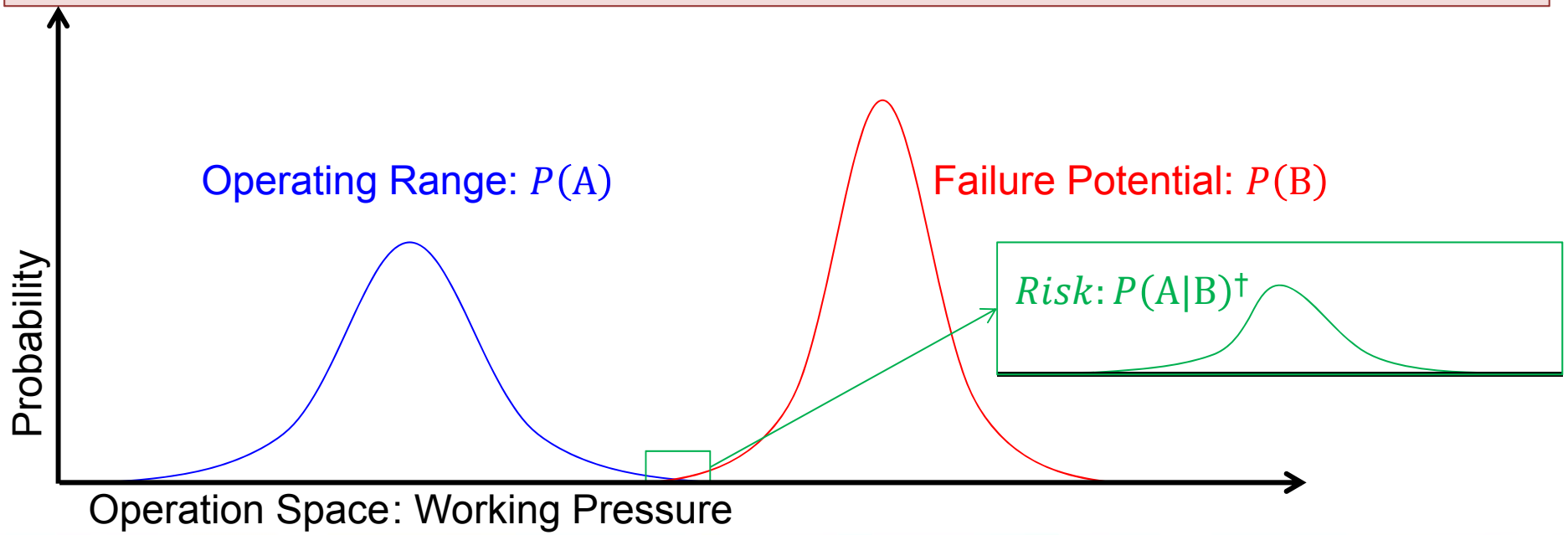

$^{\dagger}P(\mathrm{A}|\mathrm{B})$ conditional probability that event A occurs for a given event B

How best can risk management approaches incorporate H_2 behavior models?

Prescriptive vs. QRA

Both approaches work best for mature technologies with **well-established**, **data driven**, threat envelopes; however,

For limited data constraints QRA probabilities can be reduced to fundamental processes and evaluated with deterministic models.

$$Risk \propto \sum_{i,j,k} P(\text{Release}_i) P(\text{Ignition}_j | \text{Release}_i) P(\text{Hazard}_k | \text{Ignition}_j \cap \text{Release}_i) P(\text{Harm} | \text{Hazard}_k)$$

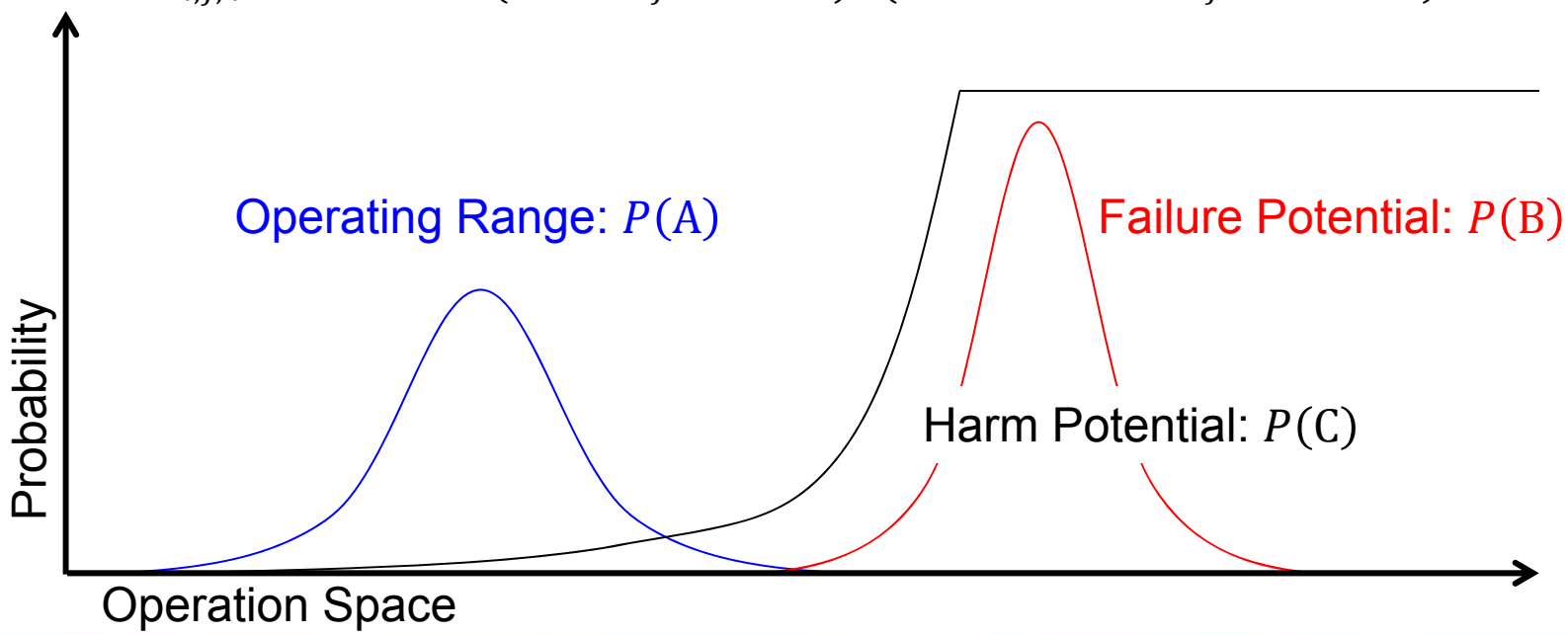

Approach:

Risk quantified by coupling validated physical modeling with stochastic scenario frequencies.

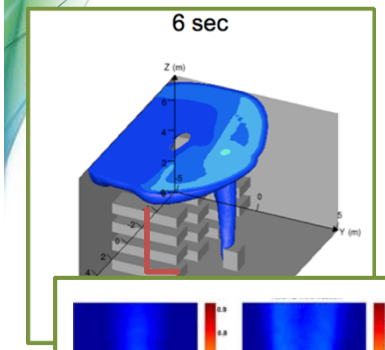

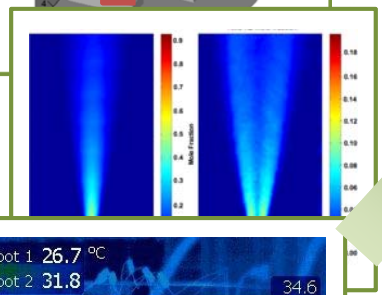

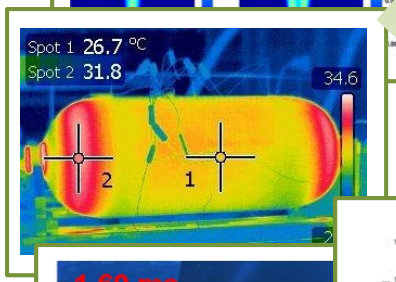

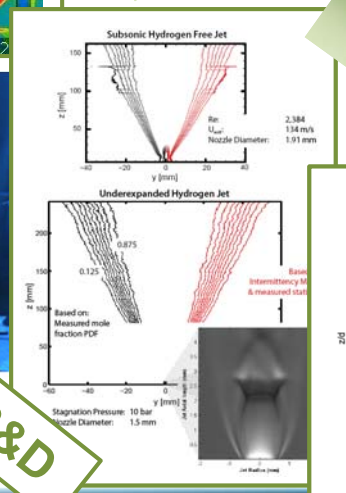

SNL H_2 SCS R&D

Dispersion
- Permeation
- Buoyant creeping flow
- Turbulent jet
- Volumetric rupture
- Fast fill protocols

Scenario Analysis/CFD Validation

Stochastic scenario frequencies: incident data, environmental/human factors, system design/mitigation

Risk

Ignition
- Ignition mechanism
- Mixture ignitability
- Ignition delay/location
- Sustained light-up

Hazard
- Flame radiation
- Overpressure (deflagration/detonation)
- O_2 dilution/depletion

Harm
- Burns
- Lung damage
- Shrapnel wounds
- Building collapse

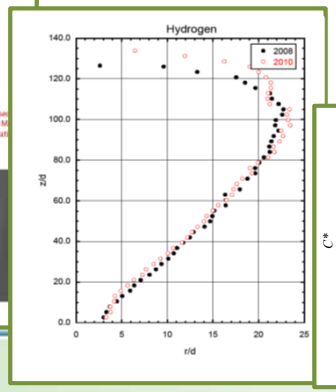

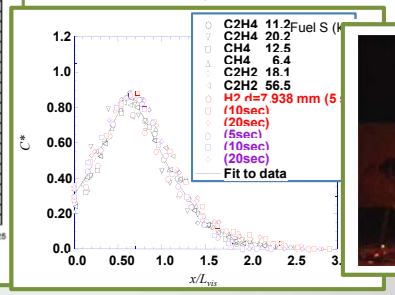

Approach:

Risk quantified by coupling validated physical modeling with stochastic scenario frequencies.

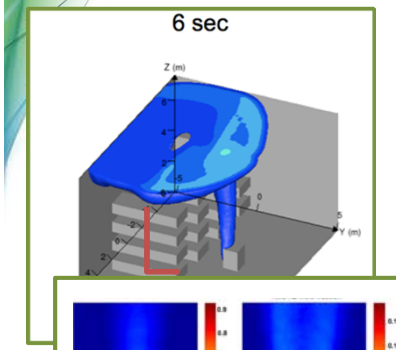

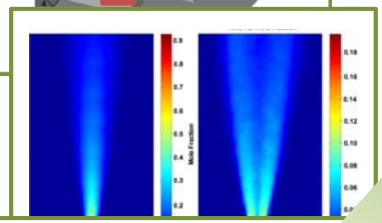

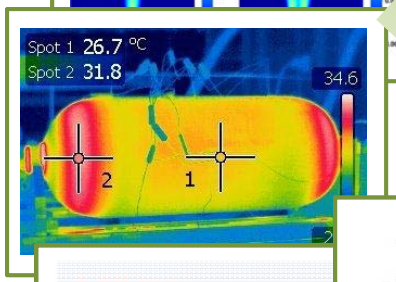

Dispersion
- Permeation
- Buoyant creeping flow
- **Turbulent jet**
- Volumetric rupture
- Fast fill protocols
- Scenario Analysis/CFD Validation

Stochastic scenario frequencies: incident data, environmental/human factors, system design/mitigation

Risk

Ignition
- Ignition mechanism
- Mixture ignitability
- Ignition delay/location
- Sustained light-up

Hazard
- Flame radiation
- Overpressure (deflagration/detonation)
- O_2 dilution/depletion

Harm
- Burns
- Lung damage
- Shrapnel wounds
- Building collapse

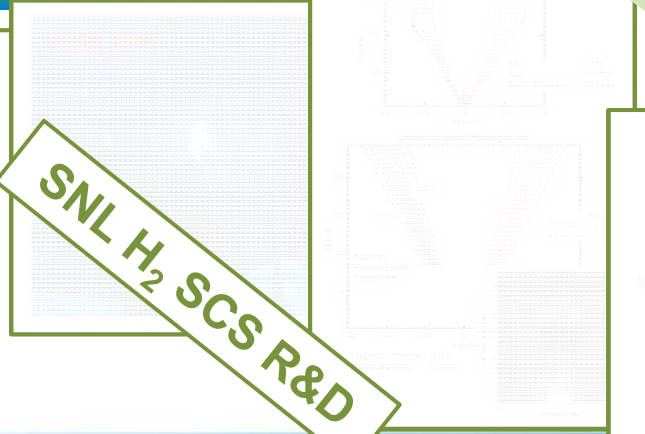

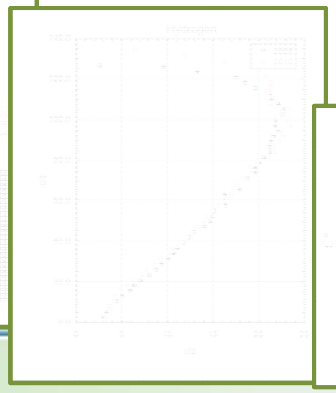

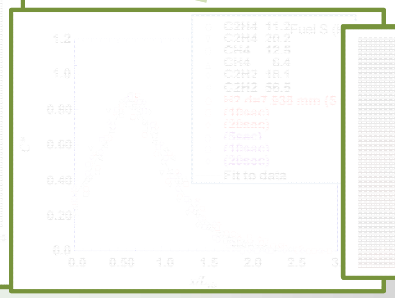

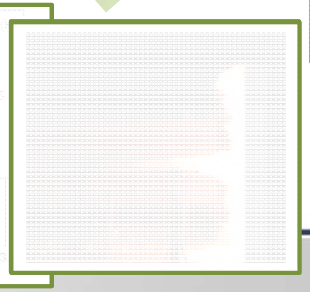

SNL H_2 SCS R&D

Plumes can be segmented into 3 primary flow regimes:

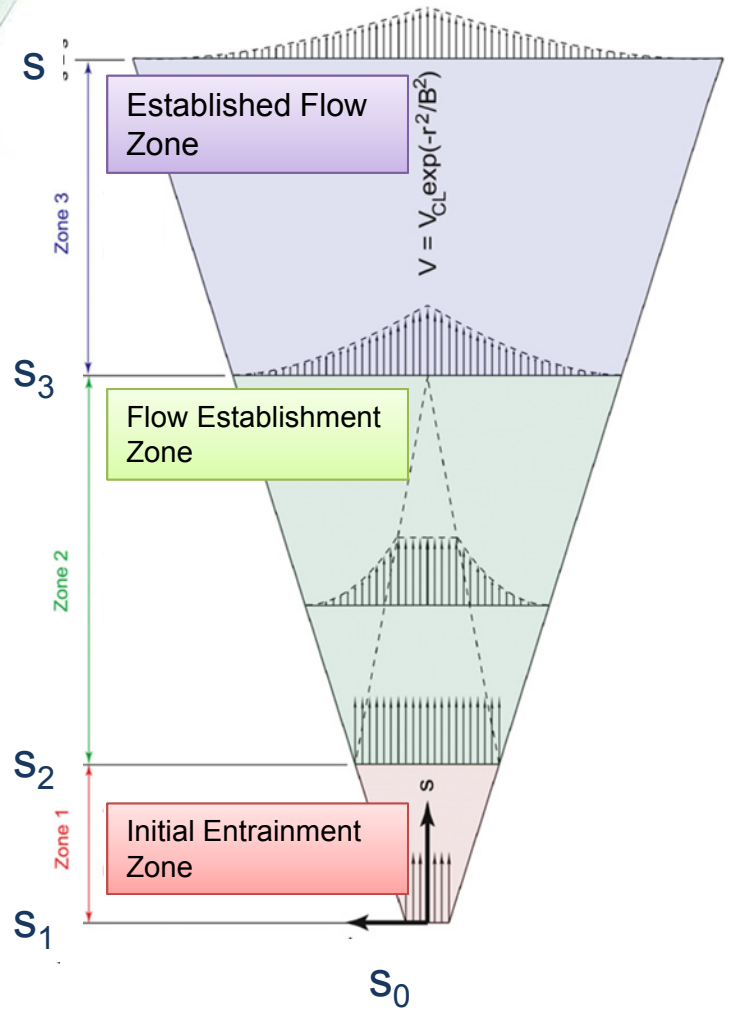

Incompressible free-jets:

$$\frac{1}{\bar{Y}_{CL}} = K_c \frac{z - z_{0Y}}{r^*} \Longrightarrow r^* = K_c \frac{z - z_{0Y}}{\bar{Y}_{CL}}$$

Where;

$\bar{Y}_{CL}$: centerline mass fraction

$r^* \equiv r_0 \sqrt{\frac{\rho_{jet}}{\rho_{air}}}$: mass weighted effective radius

K_c: centerline decay rate constant

z: axial coordinate

z_{0Y}: mass fraction virtual origin

Statistics acquired from Planar Laser Rayleigh Scatter

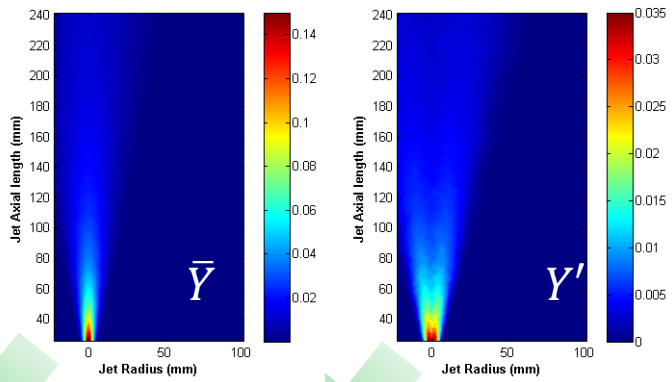

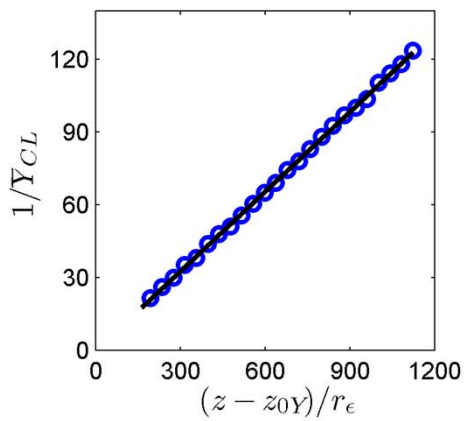

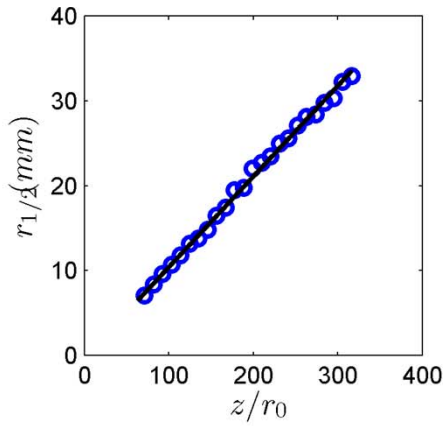

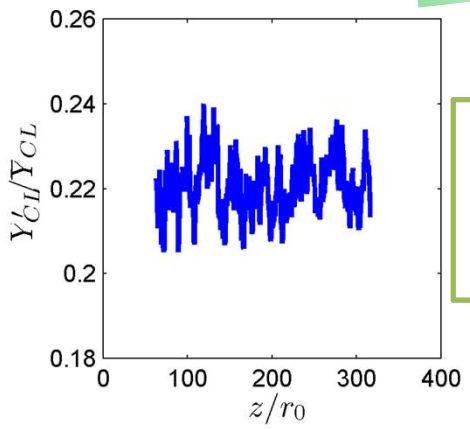

r_0	$= 0.95\ mm$
L_{pipe}	$= 250\ mm$
Q	$= 100\ lit/min$
Fr_{den}	$= 1170$

- Constant centerline decay (= 0.105) and jet spreading rates (0.113)
- Constant unmixedness ($\equiv Y'_{CL}/\bar{Y}_{CL} = 0.22$)

Centerline constants agree well with literature reported values.

Self-similarity in established flow zone require centerline values/trajectories to describe plume.

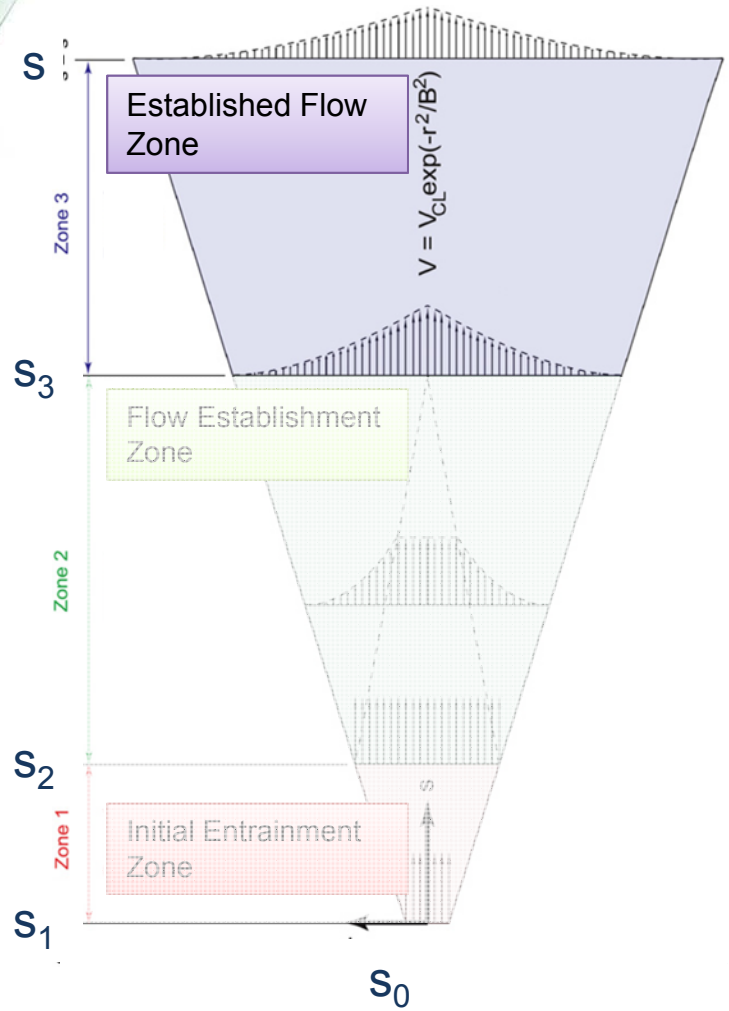

Integral plume model

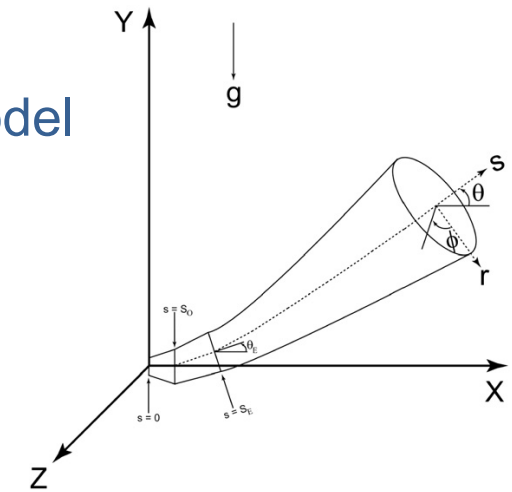

$$\frac{\partial}{\partial S}\int_0^{2\pi}\int_0^{\infty}\rho u r dr d\phi = \rho_\infty E$$

$$\frac{\partial}{\partial S}\int_0^{2\pi}\int_0^{\infty}\rho u^2 \cos\theta\, r dr d\phi = 0$$

$$\frac{\partial}{\partial S}\int_0^{2\pi}\int_0^{\infty}\rho u^2 \sin\theta\, r dr d\phi = \frac{\partial}{\partial S}\int_0^{2\pi}\int_0^{\infty}(\rho_\infty - \rho) g r dr d\phi$$

$$\frac{\partial}{\partial S}\int_0^{2\pi}\int_0^{\infty}(Y_\infty - Y) r dr d\phi = 0$$

Houf & Schefer, Int J H_2 Energy, 2008

Buoyant and momentum driven flows examined to determine appropriate entrainment rates.

Higher order statistics determined from self-similarity.

$\bar{Y} = f(\bar{Y}_{CL}, \eta)$; $Y' = g(\bar{Y}_{CL}, \eta)$

Where,

$\eta = \frac{r^*}{(r - z_{0j})}$; normalized radial

z_{0j}: momentum virtual origin

Richards and Pitts, J Fluid Mech 1993

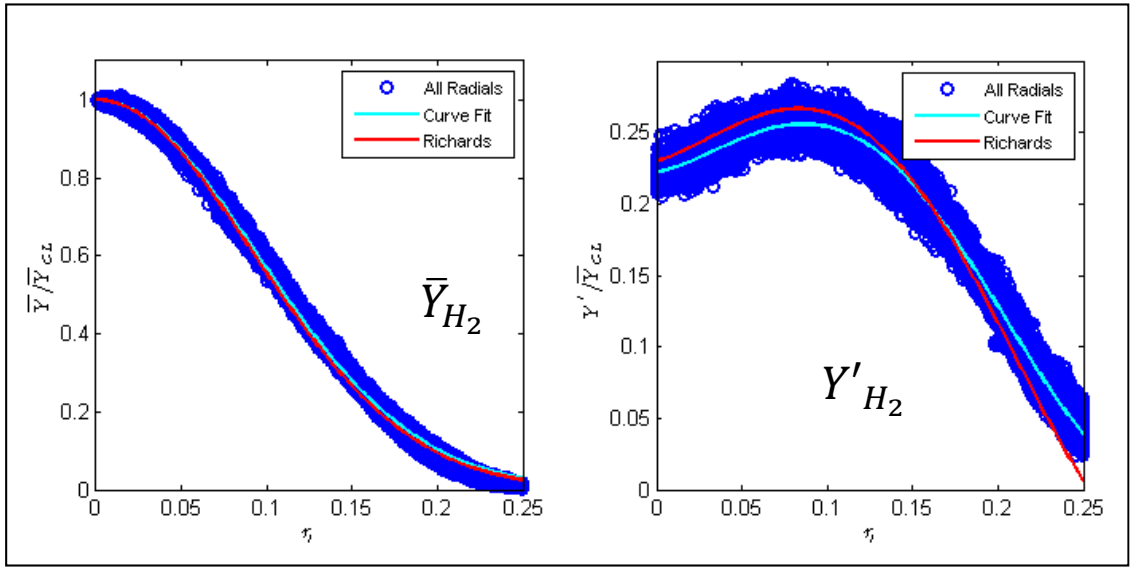

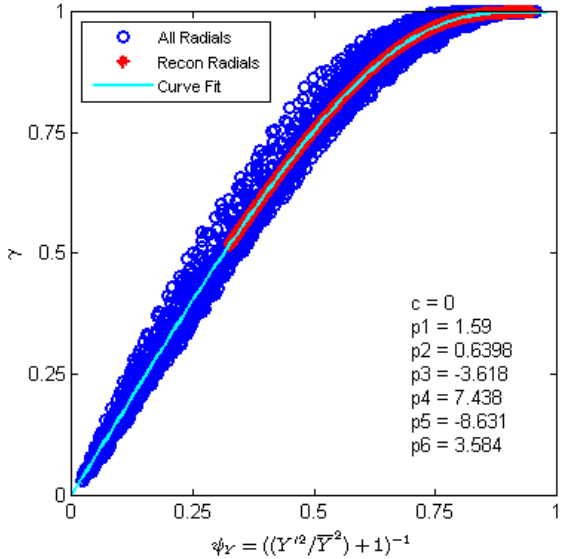

Non-linear correlation between intermittency and ratio of 1st & 2nd order statistical moments.

- Linear relationship often assumed
- **Results impact PDF prediction**

A more suitable intermittency correlating parameter is needed

Measured PDFs compared to 2 and 4 parameter Beta functions w/ constants evaluated from measured stats

$$P_C(Y_{H2}) = \frac{{Y_{H2}}^{\alpha-1}(1-Y_{H2})^{\beta-1}}{B(\alpha,\beta)}, \text{ where } \overline{Y_{H2}} = \frac{\alpha}{\alpha+\beta}, \text{ and } \overline{{Y_{H2}}'{Y_{H2}}'} = \frac{\alpha\beta}{(\alpha+\beta)^2(\alpha+\beta+1)}$$

Conditioned probability

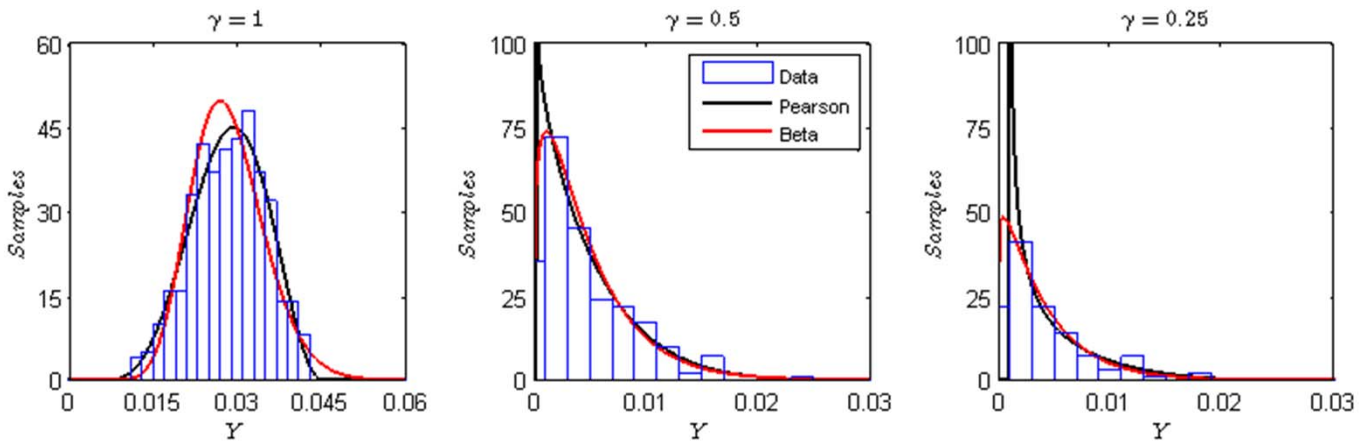

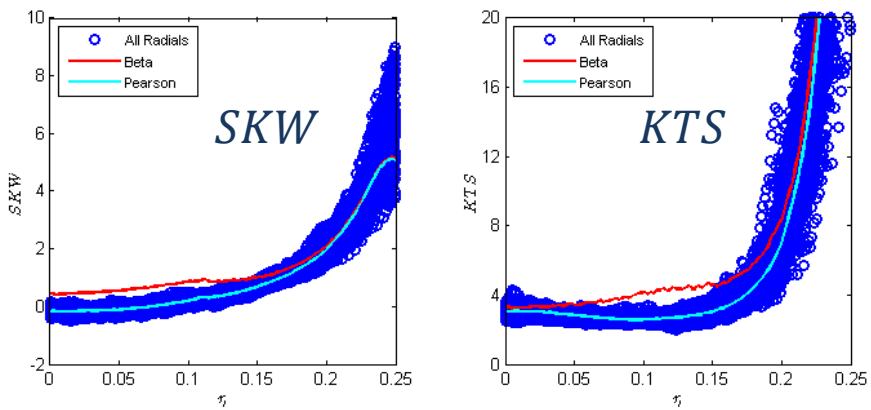

2 parameter Beta: Skewness/Kurtosis ($\eta < 0.15$), deviates from measured values.

4 parameter Beta: better matches data, but more variables needed to specify PDF bounds

No existence of H_2 jet superlayer observed

2D high resolution imaging enables turbulent length scale measurements.

$$\Lambda = \int_0^\infty \frac{\overline{Y_{H2}(x)'YH_2(x+dx)'}}{\overline{Y_{H2'}Y_{H2'}}}\,dx$$

$$\frac{1}{\lambda^2} = -\frac{1}{2}\frac{\partial^2}{\partial x^2}\left(\frac{\overline{Y_{H2}(x)'YH_2(x+dx)'}}{\overline{Y_{H2'}Y_{H2'}}}\right)$$

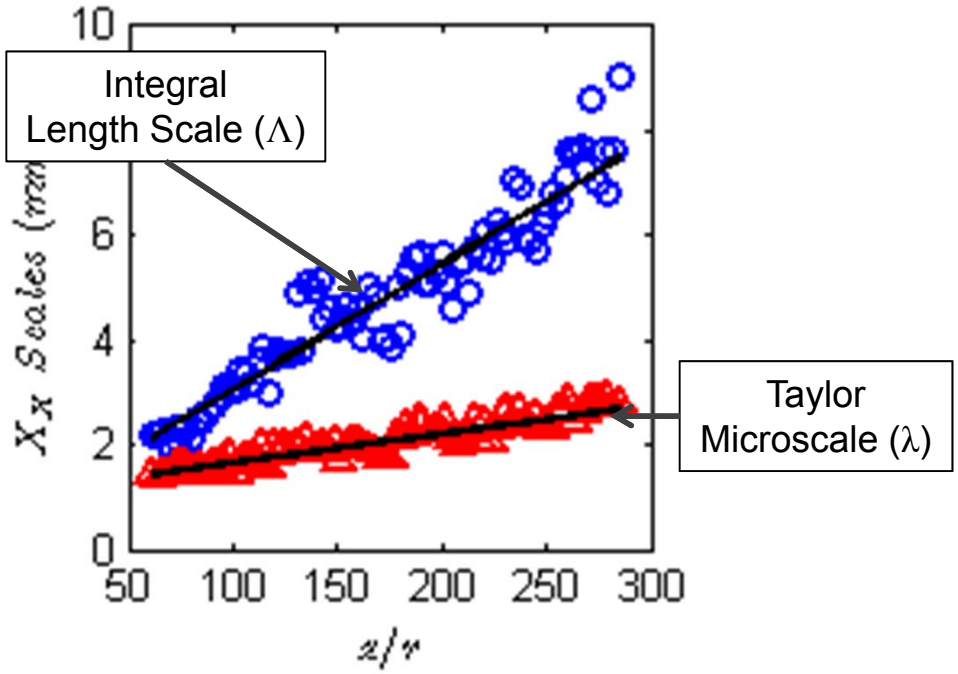

Similar integral time scales can be determined from frequency based measurements – more discussion of the relevance later.

Initial & flow establishment zones require extra modeling for different flows: choked, LH2, etc.

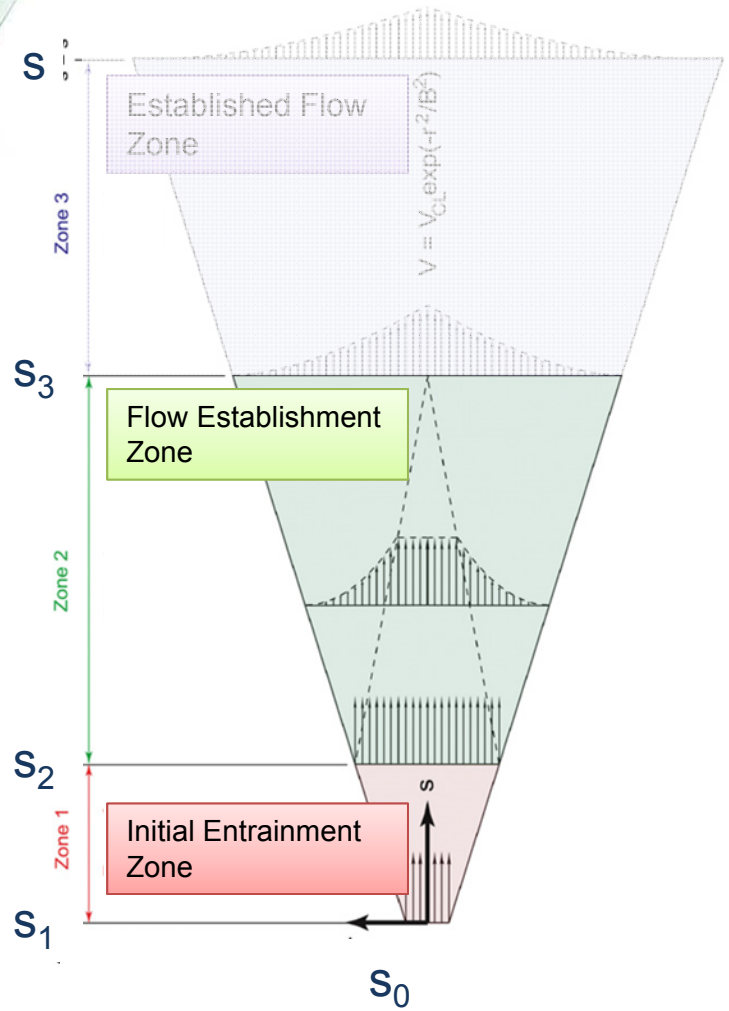

Notional Nozzle Models

Model	Conservation Equations				Critical Assumptions
	Mass	Momentum	Energy	Entropy	
Birch et al. (1984) Ruggles & Ekoto (2012)†	x		x		$T_2 = T_0$ V_2 = sonic
Ewan & Moodie (1986) Ruggles & Ekoto (2012)†	x		x		$T_2 = T_1$ V_2 = sonic
Molkov (2008)	x		x		V_2 = sonic S_1 (Abel Noble) S_2 (Ideal gas) $T_2 \approx T_1$
Birch et al. (1987) Schefer et al. (2007)†	x	x	x		$T_2 = T_0$
Yüceil & Ötügen (2002) Ruggles & Ekoto (2012)†	x	x	x		V_2 supersonic (no Mach disk)
Harstad & Bellan (2006) Winters & Houf (2008)†	x	x	x	x	All fluid passes through Mach disk

† Updated with Abel-Noble state modeling:
$p = Z\rho RH_2T;\ Z = (1 - b\rho)^{-1}$

Limited validation data available to compare model performance.

PLRS used to measure concentration statistics in isothermal region of the flow (~80 mm downstream).

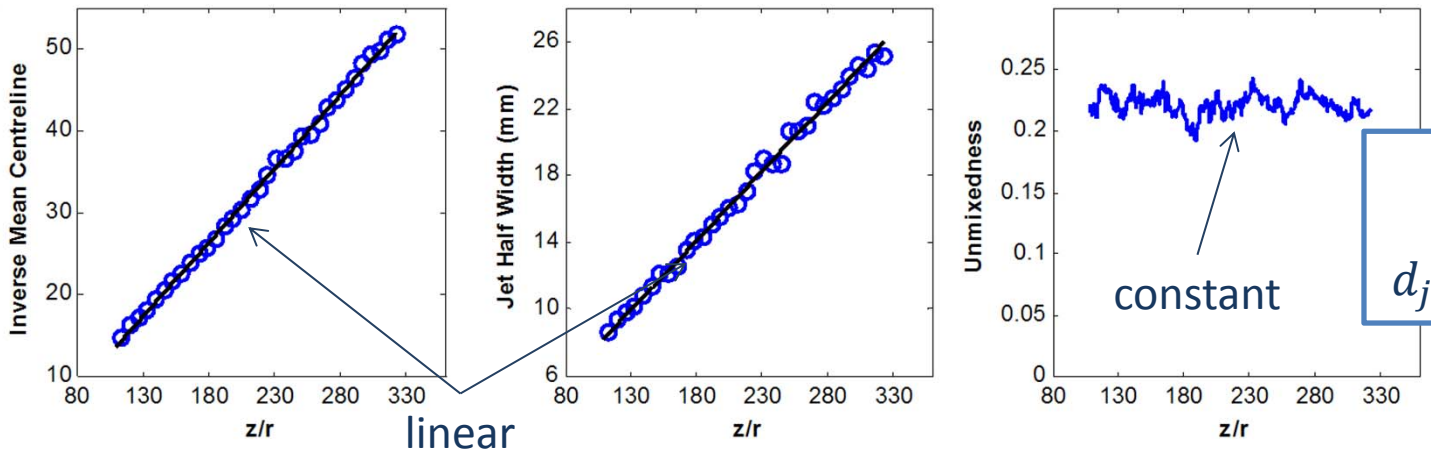

$$\frac{p_0}{p} = 10;$$
$$d_{jet} = 1.5 \text{ mm}$$

Mass weighted effective diameter fit to the data ($d^* \equiv d_{eff}\sqrt{\rho_{eff}/\rho_{air}}$)

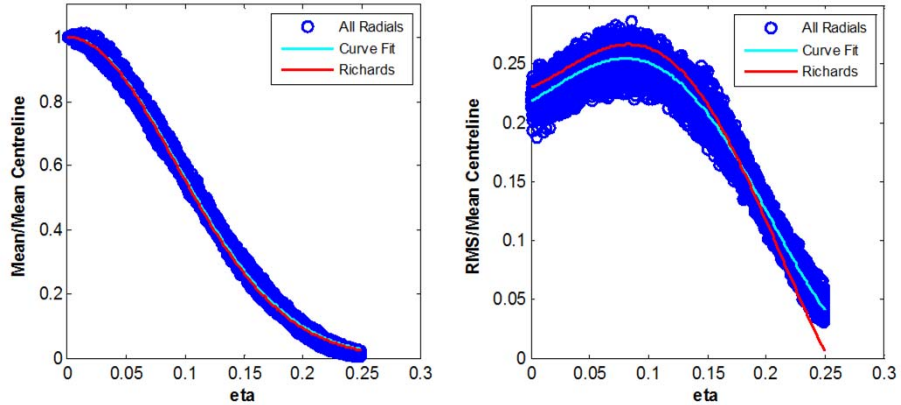

Jet statistics follow self-similarity with measured d^*

Validates notional nozzle concept and provides d^* values to assess notional nozzle model performance.

Excellent agreement observed between computed & measured mole fractions for measured *d**.

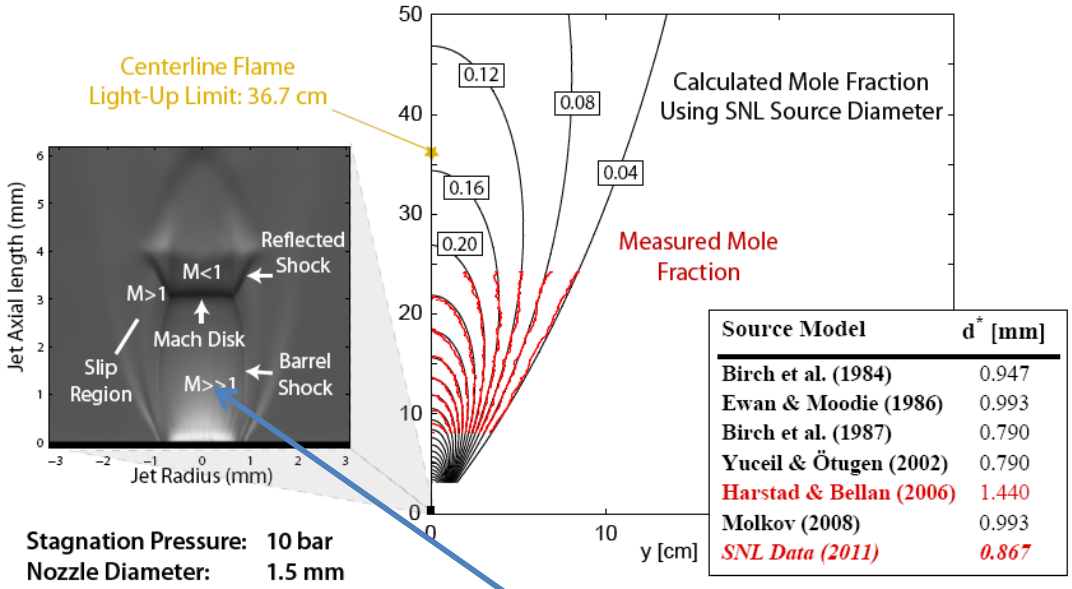

Source Model	d* [mm]
Birch et al. (1984)	0.947
Ewan & Moodie (1986)	0.993
Birch et al. (1987)	0.790
Yuceil & Ötugen (2002)	0.790
Harstad & Bellan (2006)	1.440
Molkov (2008)	0.993
SNL Data (2011)	*0.867*

Stagnation Pressure: 10 bar
Nozzle Diameter: 1.5 mm

Ruggles & Ekoto, Int J H_2 Energy, 2012.

***All models use Able-Noble EOS**

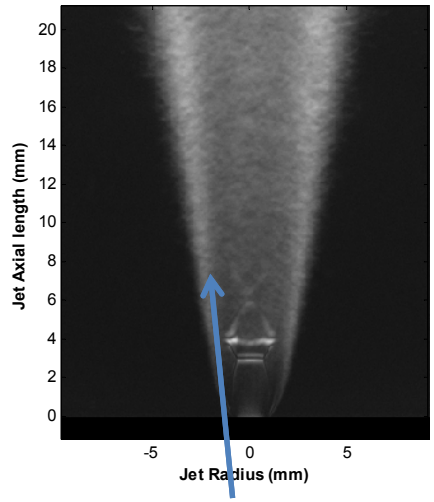

Slow shear layer growth due to compressible mixing

Papamoschou & Roshko, J Fluid Mech, 1988.

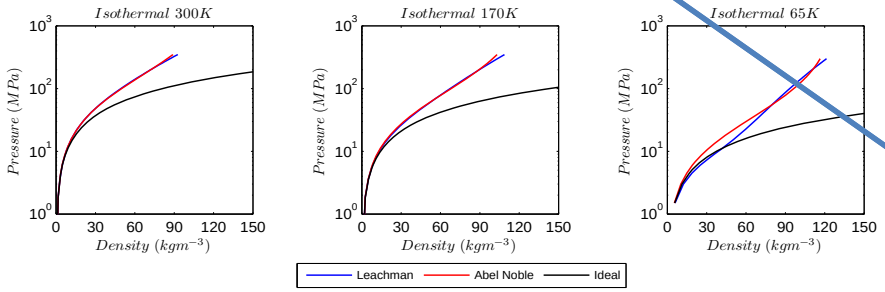

Abel-Noble EOS
- Works well at ambient *T*
- Cold states poorly predicted (T < 150 K)

Weighted pseudo sources that account for both: (1) subsonic Mach disk & (2) supersonic slip

Many leaks are non-circular:
e.g., cracks, leaky fittings, ruptures

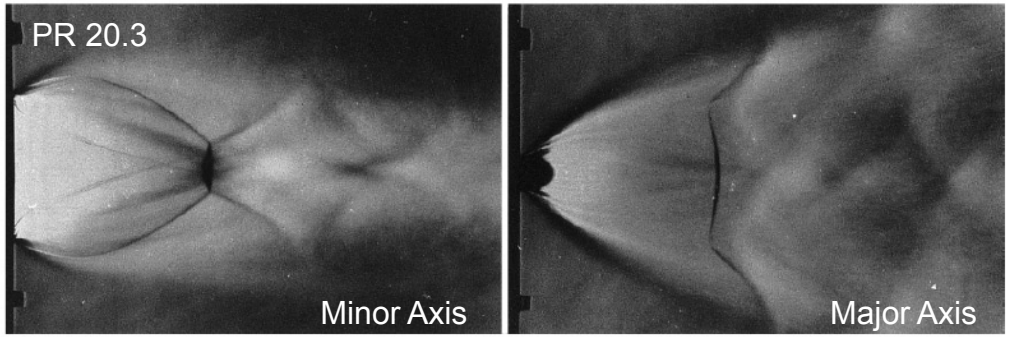

Rajakuperan & Ramaswamy, Exp in Fluids, 1998

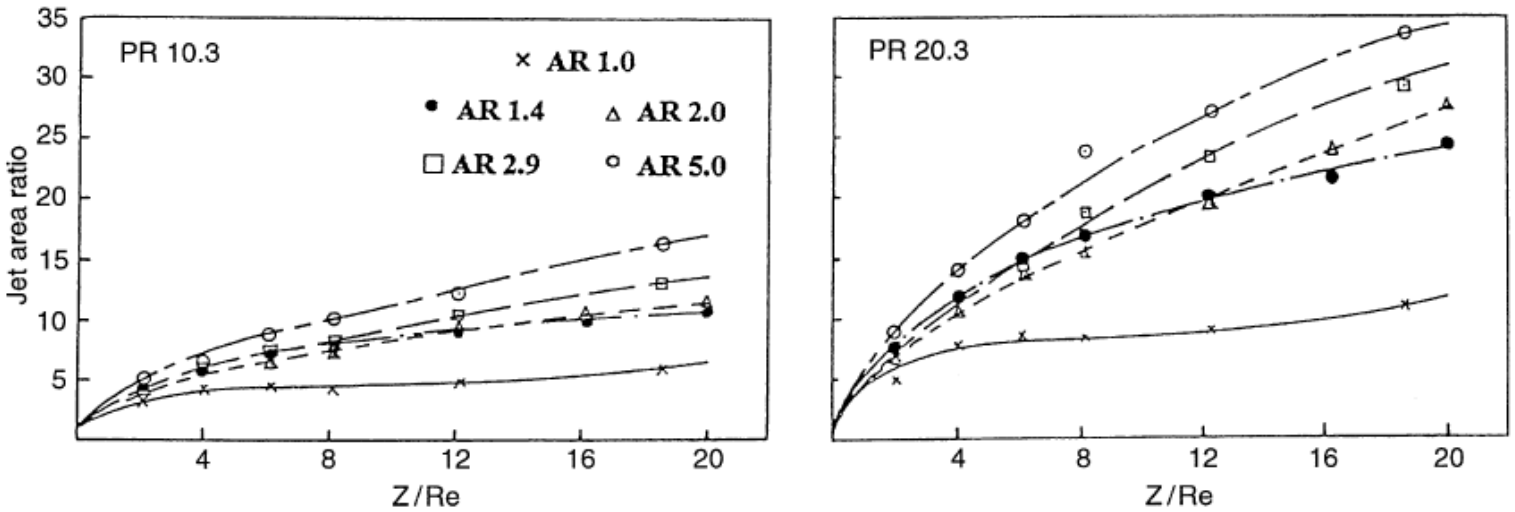

Elevated jet area ratios for high AR leaks result in faster concentration decay rates

High-fidelity validation data from H_2 jets needed to make empirical corrections is unavailable.

Integral model updated with NIST state modeling & energy conservation for LH2 plumes.

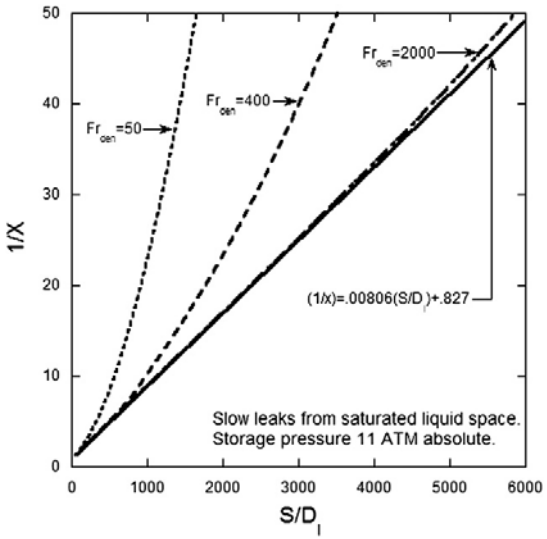

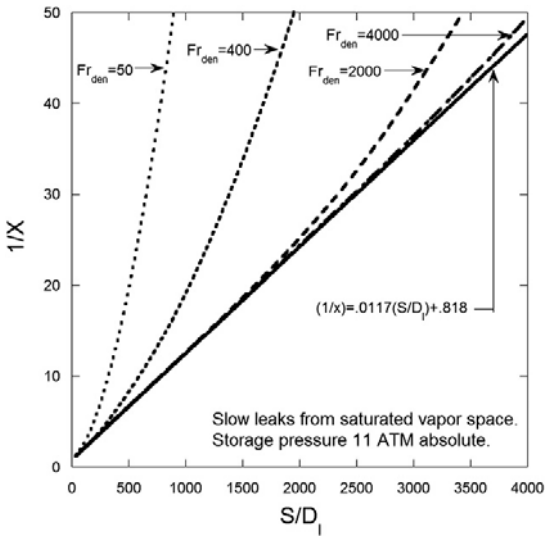

Winters & Houf, Int J H_2 Energy, 2011.

Saturated Vapor Leak[1]		
Pipe ID (mm)	Leak Diameter[4] (mm)	Distance[5] (m)
6.35 mm (1/4 in)	1.100	4.431
12.7 mm (1/2 in)	2.200	8.861
19.05 mm (3/4 in)	3.299	13.29
25.4 mm (1 in)	4.399	17.71
31.75 mm (1.25 in)	5.499	22.13
38.10 mm (1.5 in)	6.599	26.55
44.45 mm (1.75 in)	7.699	30.96
50.80 mm (2 in)	8.799	35.36

Saturated Liquid Leak[2]		
Pipe ID (mm)	Leak Diameter[4] (mm)	Distance[5] (m)
6.35 mm (1/4 in)	1.100	5.659
12.7 mm (1/2 in)	2.200	11.26
19.05 mm (3/4 in)	3.299	16.75
25.4 mm (1 in)	4.399	22.11
31.75 mm (1.25 in)	5.499	27.31
38.10 mm (1.5 in)	6.599	32.37
44.45 mm (1.75 in)	7.699	37.29
50.80 mm (2 in)	8.799	42.06

Subcooled Liquid Leak[3]		
Pipe ID (mm)	Leak Diameter[4] (mm)	Distance[5] (m)
6.35 mm (1/4 in)	1.100	9.611
12.7 mm (1/2 in)	2.200	15.9
19.05 mm (3/4 in)	3.299	21.94
25.4 mm (1 in)	4.399	27.64
31.75 mm (1.25 in)	5.499	33.09
38.10 mm (1.5 in)	6.599	38.34
44.45 mm (1.75 in)	7.699	43.46
50.80 mm (2 in)	8.799	48.4

Distance to 4% H_2 Mole Fraction from a 3% leak
(Model validation limited to 80 K jet release data from KIT)

Additional validation data needed at more relevant temperatures.

Approach:

Risk quantified by coupling validated physical modeling with stochastic scenario frequencies.

Dispersion
- Permeation
- Buoyant creeping flow
- Turbulent jet
- Volumetric rupture
- Fast fill protocols
- Scenario Analysis/CFD Validation

Stochastic scenario frequencies: incident data, environmental/human factors, system design/mitigation

Ignition
- **Ignition mechanism**
- **Mixture ignitability**
- Ignition delay/location
- **Sustained light-up**

Risk

Hazard
- Flame radiation
- Overpressure (deflagration/detonation)
- O_2 dilution/depletion

Harm
- Burns
- Lung damage
- Shrapnel wounds
- Building collapse

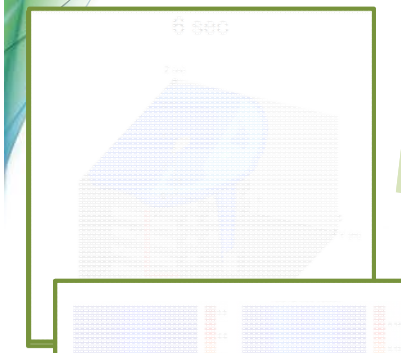

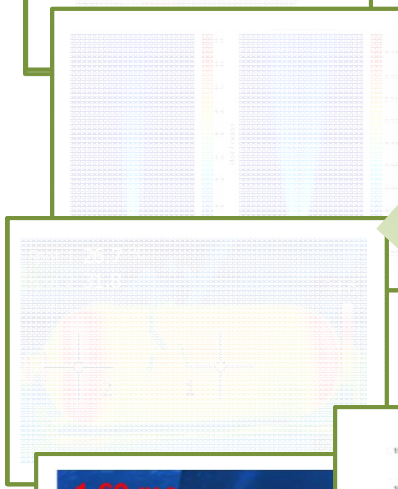

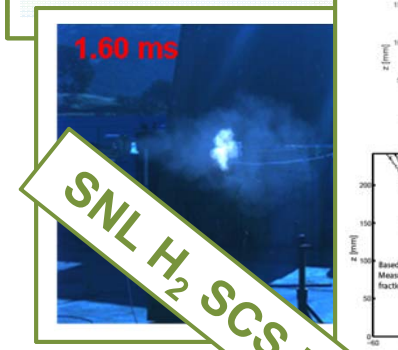

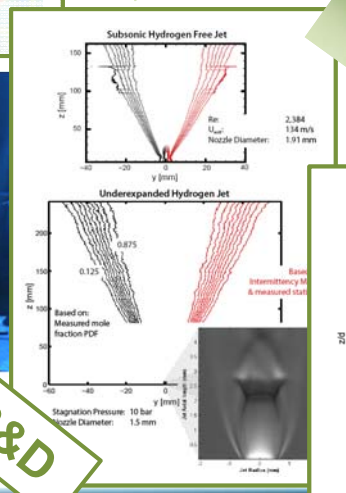

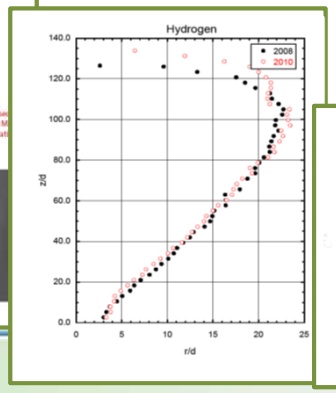

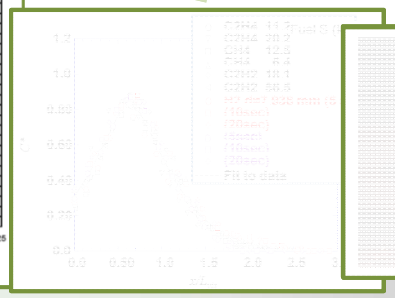

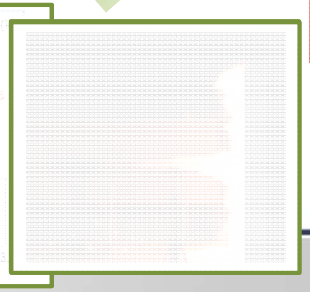

SNL H_2 SCS R&D

Electrostatic discharge (ESD) from entrained charged particles.

Low H_2 minimum ignition energy (~0.02 mJ)

Sample B
Iron (III) Oxide
Fe_2O_3

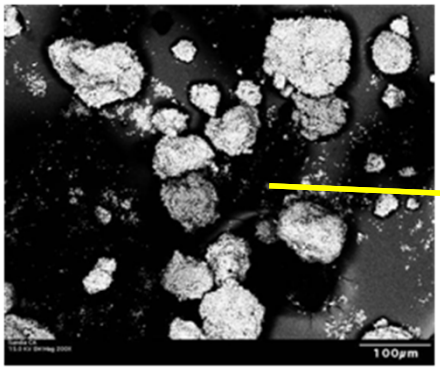

200x

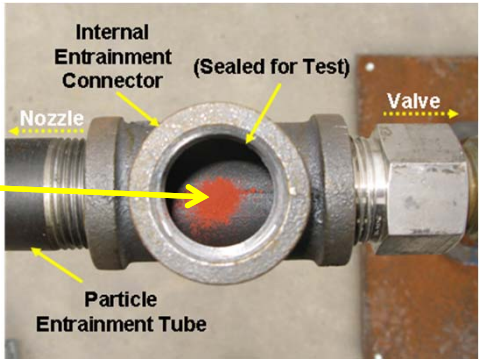

Repeatable ignitions from spark discharges between isolated conductors.

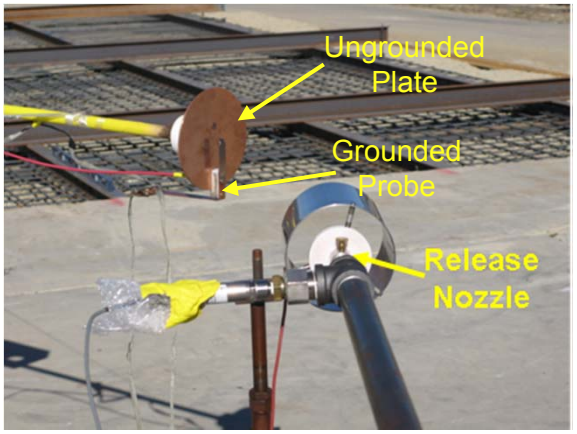

Merillo et al., Proc ICHS, 2011

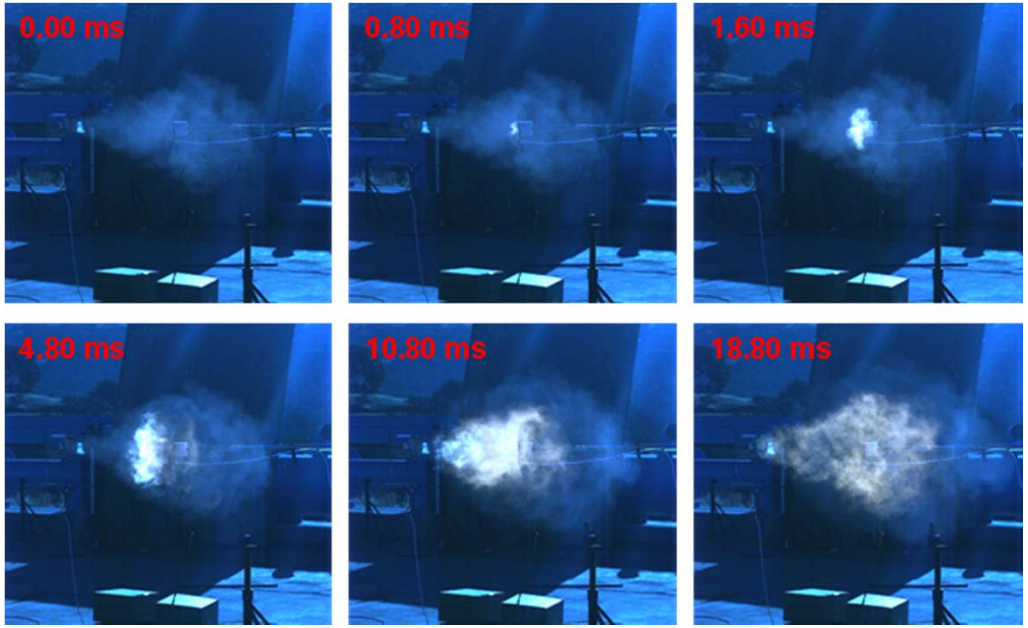

Modeling ESD requires particle information (size, number, type) along with modeled spark discharge behavior.

Flammability Factor maps from concentration statistics agree well with laser-spark ignition probabilities.

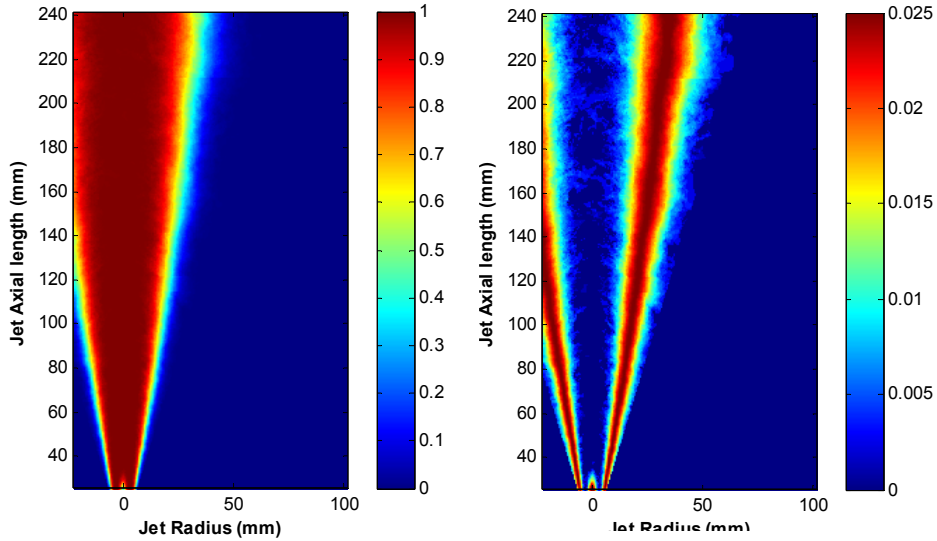

$$FF = \sum \left(\int_{LFL}^{UFL} \chi_{H_2} = 1 \right) \times \frac{1}{n}$$

Schefer et al., Int J H2 Energy, 2011

D = Ø1.901mm

Flow = 100slm H_2

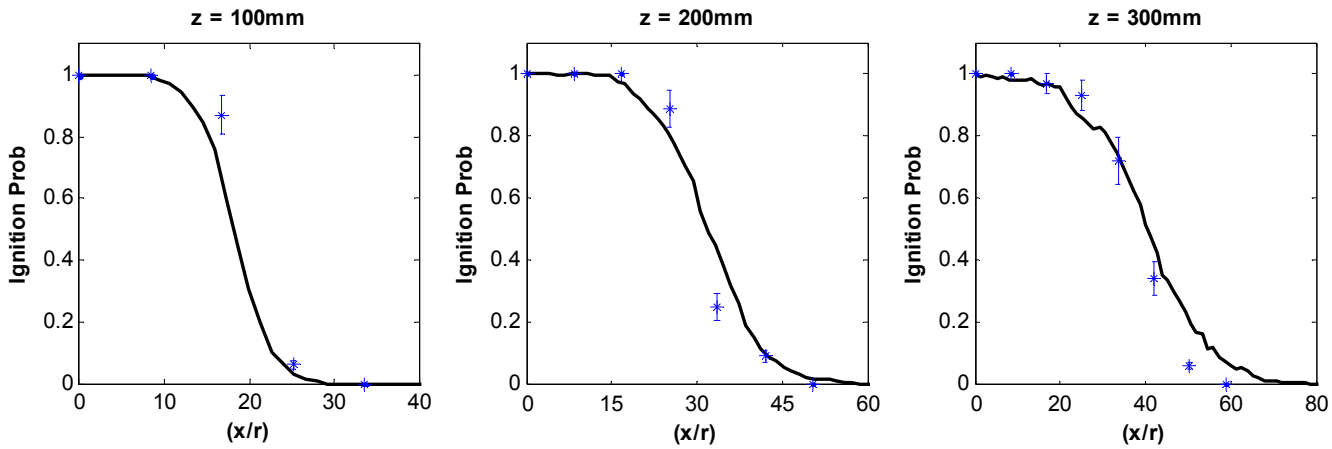

Prediction of FF depends only on prediction of PDF.

Several methods have been developed to model the transition of incipient ignition to sustained light-up.

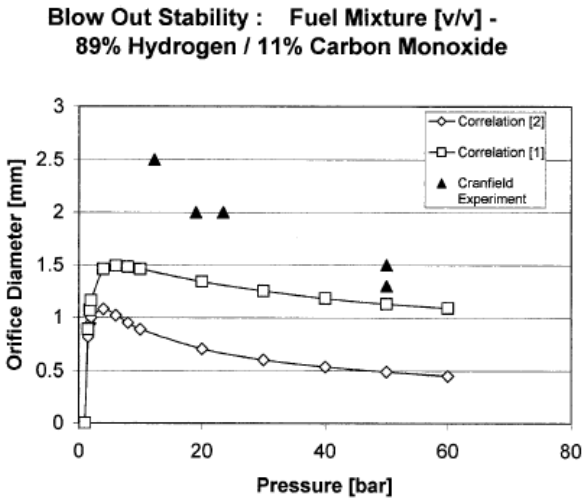

Devaud et al., Shock Waves, 2002

$$U_b = 0.017 \cdot RH\,(1 - 3.5 \cdot 10^{-6} RH)$$

$$RH = \left[\frac{4}{\bar{Y}_s}\left(\frac{\rho_{eff}}{\rho_\infty}\right)^{\frac{1}{2}} + 5.8\right]\frac{S_u d_{eff}}{\upsilon_e}$$

Kalghatgi, Combust Sci Tech, 1981
Birch et al., Combust Sci Tech, 1988

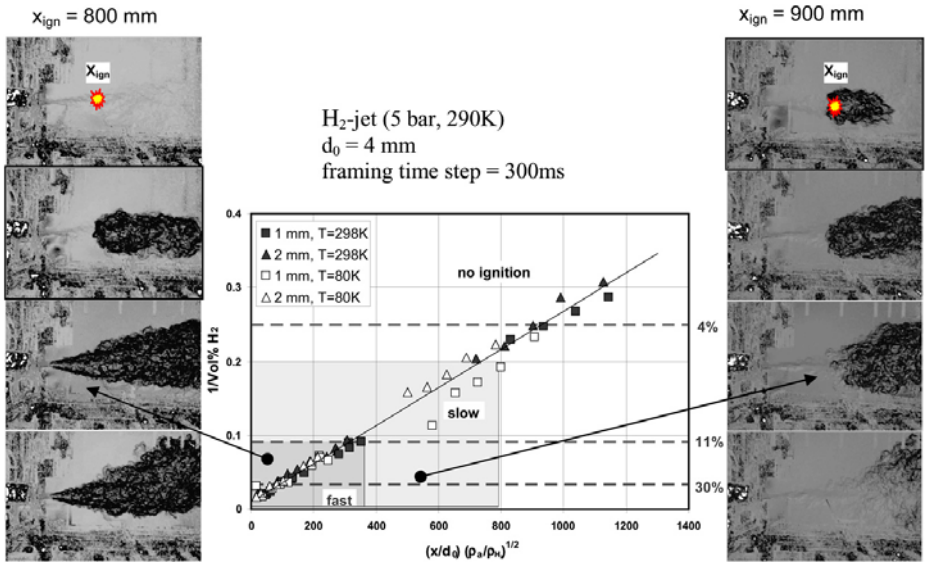

Veser et al., Int J H2 Energy, 2011

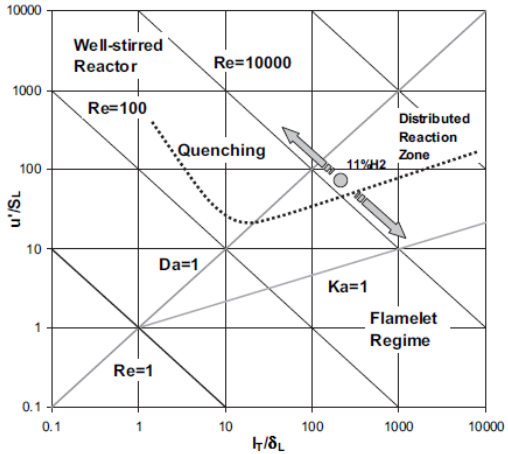

$$U_b = 1.7 S_t \qquad S_t = 0.875 Ka^{0.392} u'$$

$$Ka = 0.157\left(\frac{u'}{S_u}\right)^2 Re_L^{-0.5}$$

Burgess & Lawn, Combust Flame, 1999

Amount of available data is still too sparse to develop a complete empirical correlation.

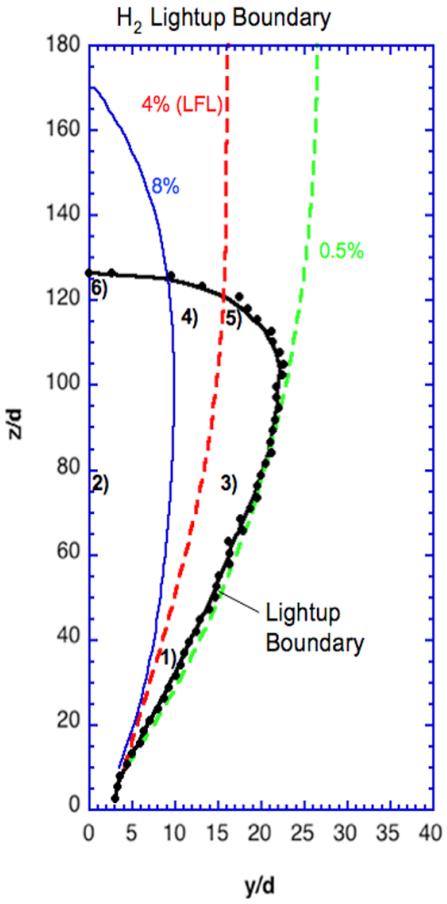

Schefer et al., Int J H2 Energy, 2011

1.91 mm diam.
26 lit/min

A phenomenological approach has been adopted by SNL

1.91 mm diam.
100 lit/min

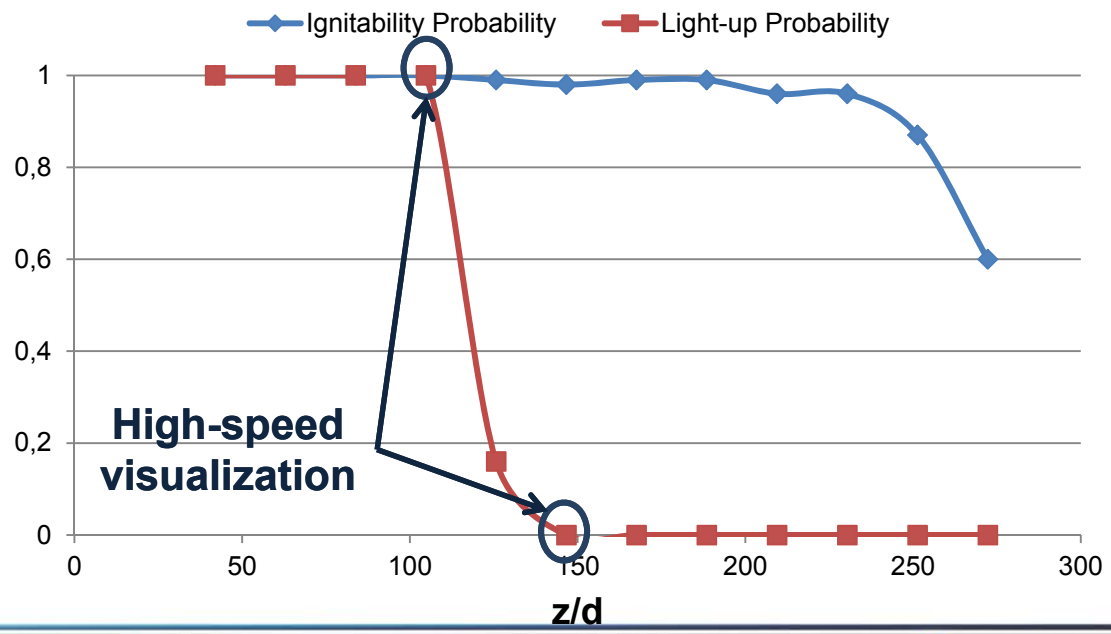

High-speed ignition imaging elucidates light-up mechanisms & confirms validity of flamelet approach.

Ignition w/ light-up

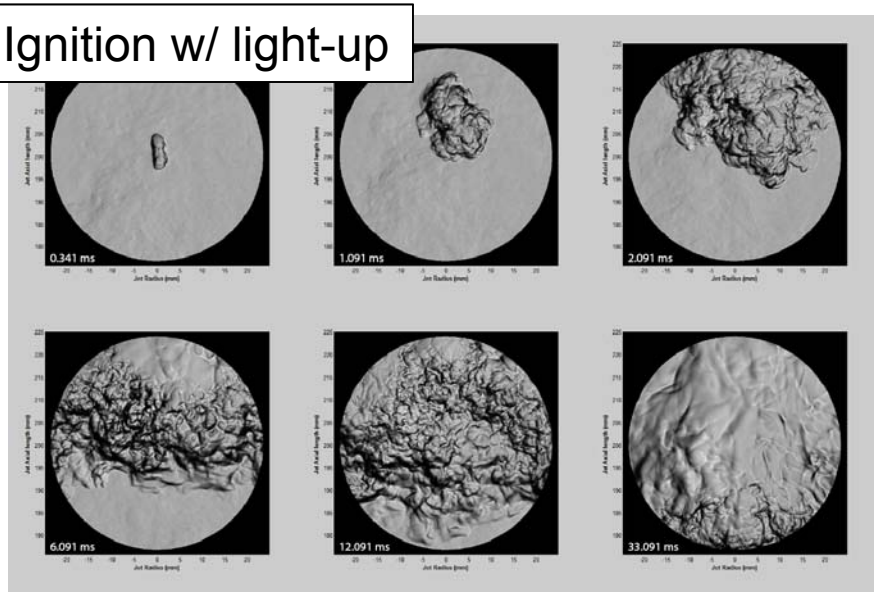

Ignition w/o light-up

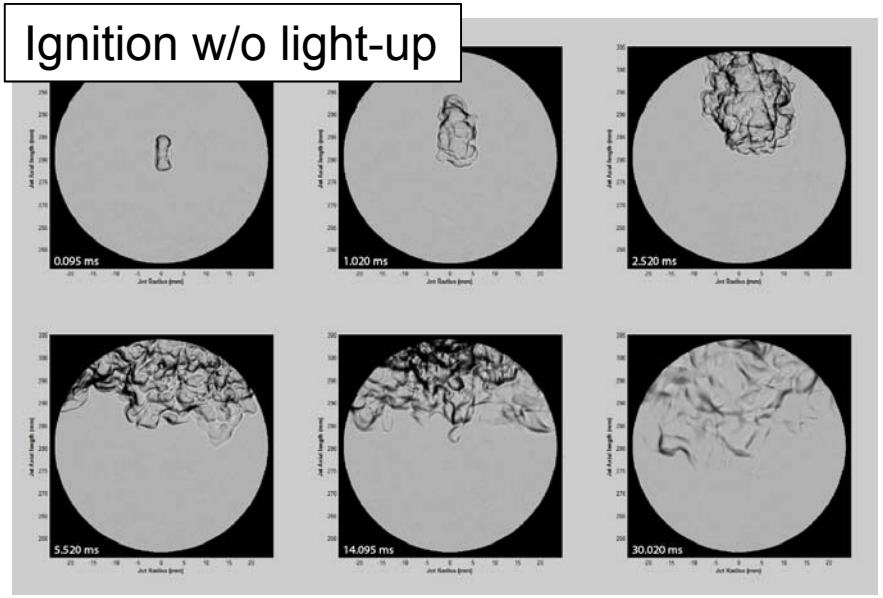

New acetone seeded LIF diagnostic enables **turbulent mixing measurements**

Turbulent diffusion primarily controls mixing in non-reacting jets

For non-reacting H_2/air mixtures:

$$\rho = Y_{H_2}\rho_{H_2} + \left(1 - Y_{H_2}\right)\rho_{air}$$

$$D_{turb} \equiv \frac{1}{\nabla \bar{Y}_{H_2}} \cdot \left[\overline{\boldsymbol{u}' Y_{H_2}'} + \frac{\bar{\boldsymbol{u}}}{\bar{\rho}}\overline{\rho' Y_{H_2}'} + \frac{\bar{Y}_{H_2}}{\bar{\rho}}\overline{\rho' \boldsymbol{u}'} + \frac{1}{\bar{\rho}}\overline{\boldsymbol{u}' \rho' Y_{H_2}'}\right]$$

Coupled velocity/concentration statistics

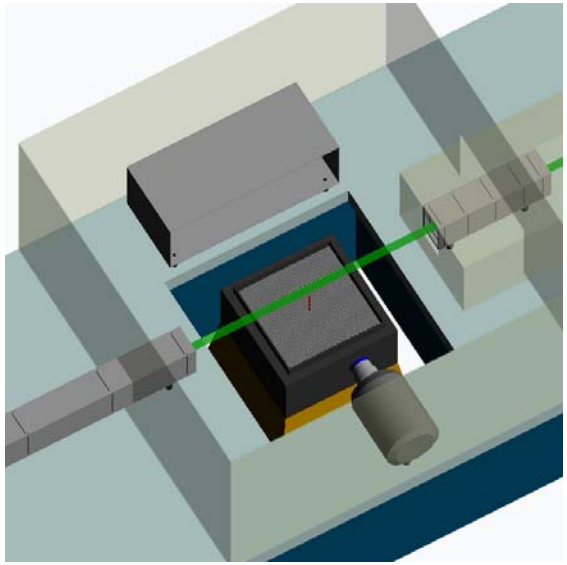

Measurements to be coupled with OH LIF and used to conditionally sample velocity/scalar fields around developing ignition kernels.

Approach:

Risk quantified by coupling validated physical modeling with stochastic scenario frequencies.

Dispersion
- Permeation
- Buoyant creeping flow
- Turbulent jet
- Volumetric rupture
- Fast fill protocols
- Scenario Analysis/CFD Validation

Stochastic scenario frequencies: incident data, environmental/human factors, system design/mitigation

Ignition
- Ignition mechanism
- Mixture ignitability
- Ignition delay/location
- Sustained light-up

Risk

Hazard
- **Flame radiation**
- **Overpressure** (deflagration/detonation)
- O_2 dilution/depletion

Harm
- Burns
- Lung damage
- Shrapnel wounds
- Building collapse

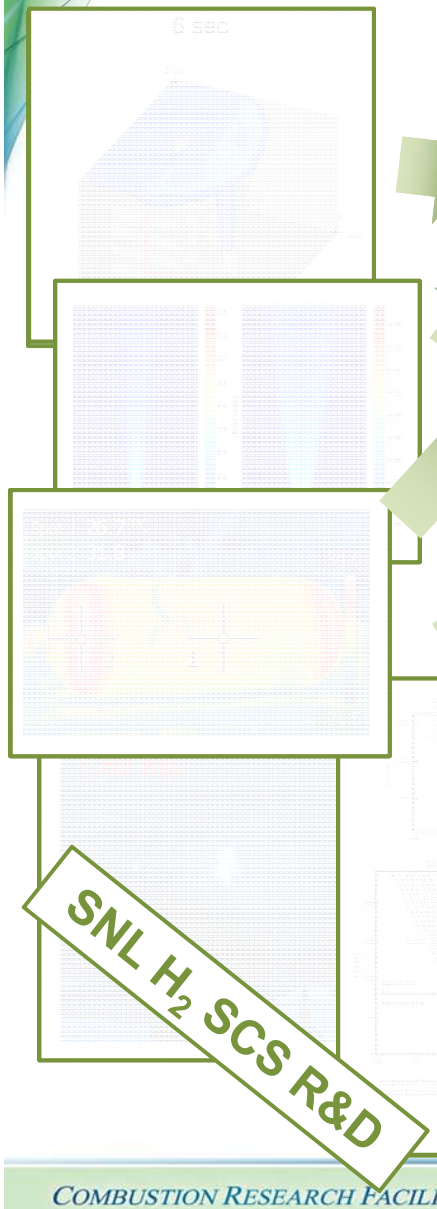

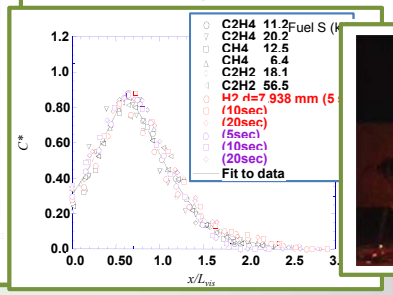

SNL H_2 SCS R&D

Empirical methods exist to model small to medium-scale H_2 flame radiation boundaries.

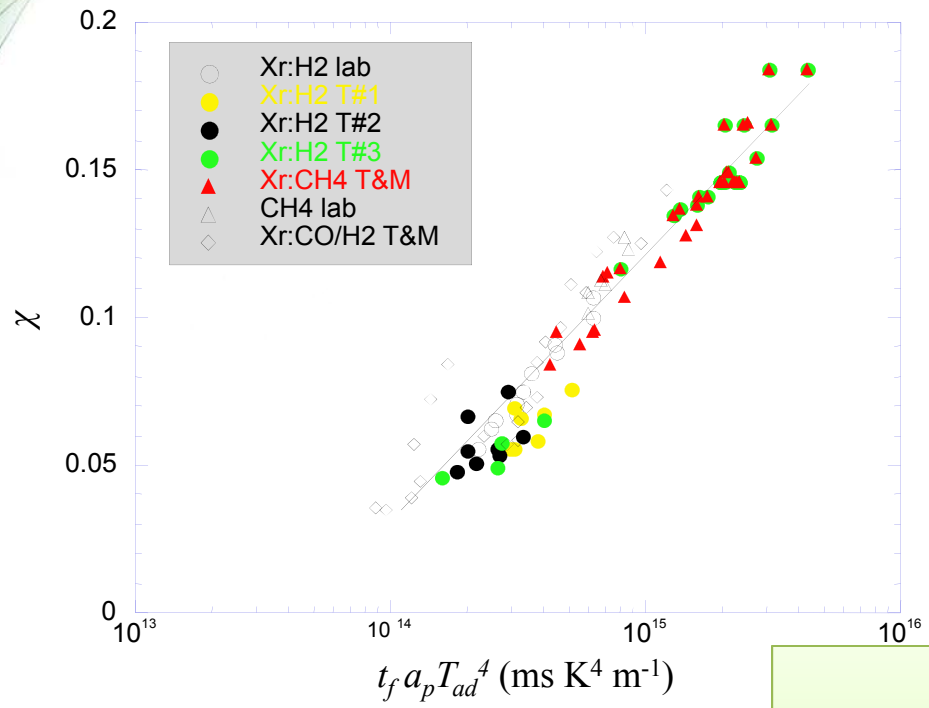

$$\chi = 0.08916 \cdot log_{10}\left(t_f a_p T_{ad}^4\right) - 1.2172$$

a_p : plank-mean absorption [m^{-1}]
T_{ad} : adiabatic flame temperature [K]

Molina et al, Proc Comb Inst (2007)

$$\chi = \frac{A_f}{VF \cdot \tau} \cdot \frac{q}{\dot{m} \cdot \Delta H_c}$$

χ : Radiant fraction
A_f : Flame surface area [m^2]
VF : View factor
τ : Atmospheric transmissivity
q : Radiative heat flux [kW/m^2]
$\dot{m}$: Fuel mass flow rate [kg/s]
ΔH_c : Heat of combustion [kJ/kg]

$$t_f = \frac{m}{\dot{m}}$$

t_f : Flame residence time [ms]
m : Flame mass [kg]

Only validated for flame lengths < 10 m

Radiant fractions derived from radiative heat flux measurements from strategically placed radiometers.

Jet	d_j [mm]	$\dot{m}$ [kg/s]	L_f [m]	p_0 [barg]	T_0 [K]	RH [%]	T_{amb} [K]	p_{amb} [mbar]	U_{wind} [m/s]	Wind dir [°]
1	20.9	1.0	17.4	59.8	308.7	94.3	280	1022	2.84	68.5
2	52.5	7.4	48.5	62.1	287.8	94.5	280	1011	0.83	34.0

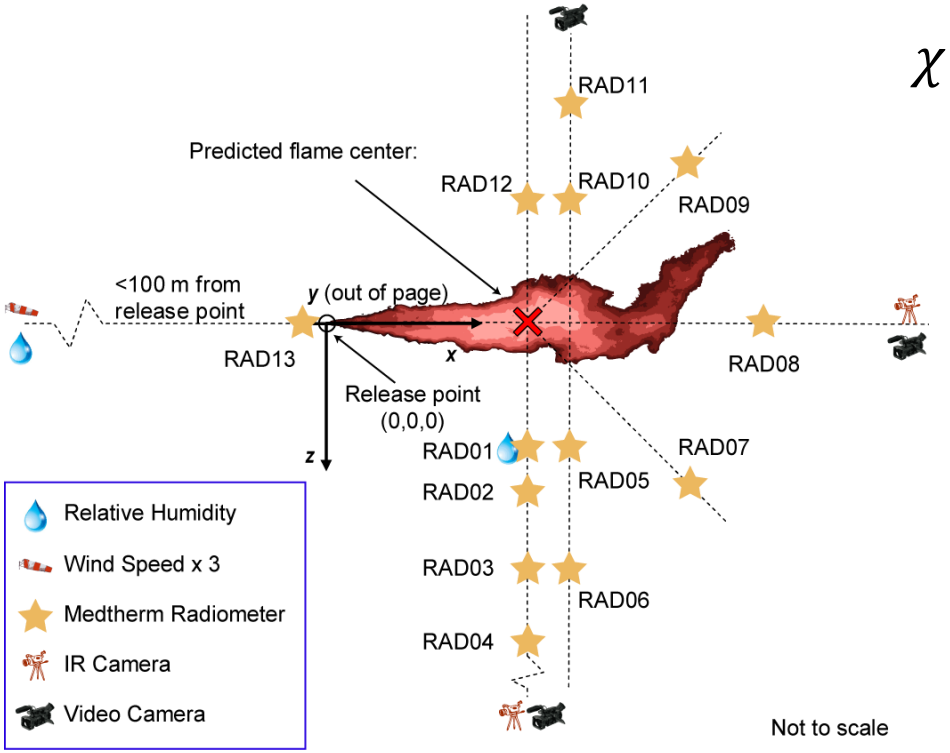

$$\chi \propto t_f a_p T_{ad}^4$$

For Hydrogen:
a_p = 0.23 [m^{-1}]
T_{ad} = 2390 K
ΔH_c = 119 MJ/kg

$$\chi = \frac{A_f}{VF \cdot \tau} \cdot \frac{q}{\dot{m} \cdot \Delta H_c}$$

Where,

$$\frac{A_f}{VF \cdot \tau} \approx \frac{4\pi R^2}{C^*}$$

Sivathanu & Gore, Combust Flame (1993)

$$t_f = \frac{m}{\dot{m}}$$

Where,

$$m \approx \frac{\pi}{12} \rho_f W_f^2 L_f y_s$$

Turns & Myhr, Combust Flame (1991)

R: Radial distance [m]
C^*: Non-dimensional radiant power
L_f / W_f: Flame length/width [m]
ρ_f: Flame density [kg/m^3]
y_s: Stoichiometric mass fraction

Non-dimensional radiant power determined using single source model with an exponential shape factor.

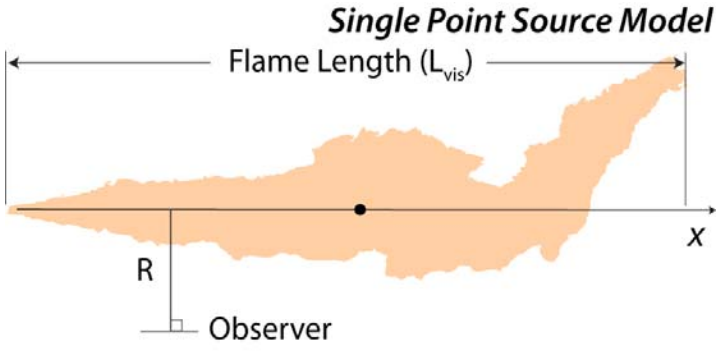

Sivathanu & Gore, Combust Flame, 1993

$$\chi = \frac{A_f}{VF \cdot \tau} \cdot \frac{q}{\dot{m} \cdot \Delta H_c}$$

Where,

$$\frac{A_f}{VF \cdot \tau} \approx \frac{4\pi R^2}{C^*}$$

unknown

$$C^*_{SPS} \approx 0.85985 \cdot exp\left(-2.7579 \cdot \left|\frac{x}{L_f} - 0.6352\right|\right) \cdot \tau$$

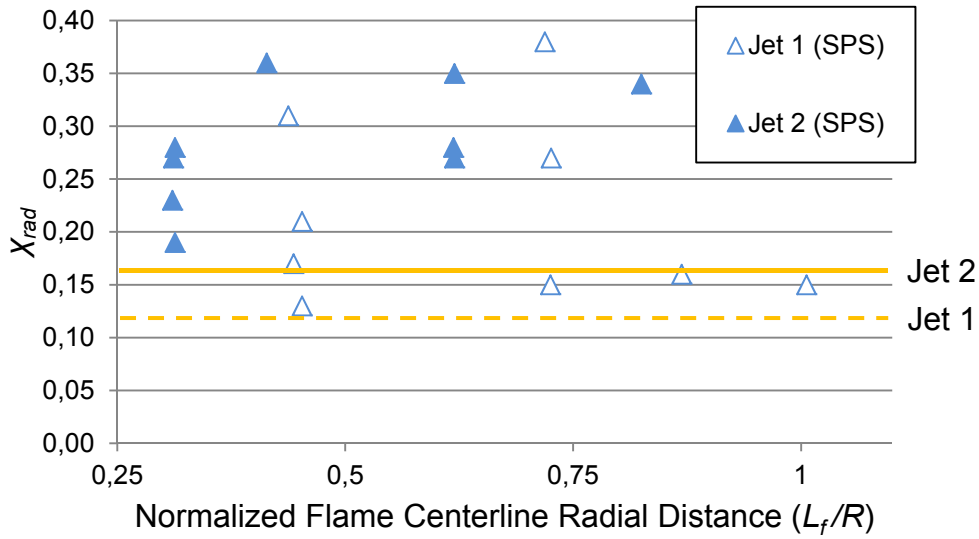

Large spread in single-point source computed radiant fractions from measured heat fluxes.

Measured radiant fraction values were ***~80% higher*** than predictions based on flame residence time correlations.

Smaller spread in radiant fraction data & better agreement with residence time correlations.

Jet	d_j [mm]	$\dot{m}$ [kg/s]	L_f [m]	p_0 [barg]	T_0 [K]	RH [%]	T_{amb} [K]	p_{amb} [mbar]	U_{wind} [m/s]	Wind dir [°]
1	20.9	1.0	17.4	59.8	308.7	94.3	280	1022	2.84	68.5
2	52.5	7.4	48.5	62.1	287.8	94.5	280	1011	0.83	34.0

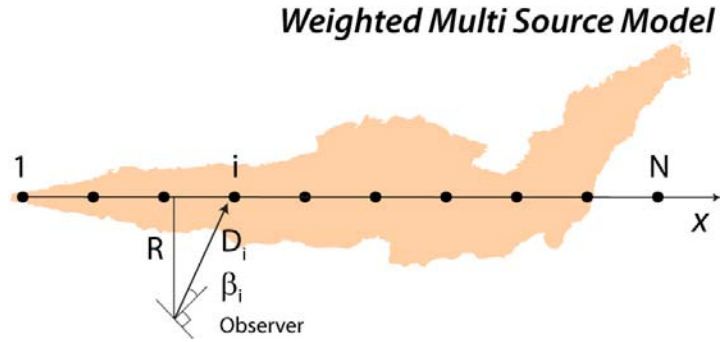

Hankinson & Lowesmith, Combust Flame, 2012

$$C^*_{WMS} = R^2 \sum_{i=1}^{N} \frac{w_i \cos \beta_i}{D_i^2} \tau_i$$

D_i: Distance from observer to source point i
β_i: Angle between observer normal and vector $\mathbf{D_i}$
w_i: Weight factor for source point i

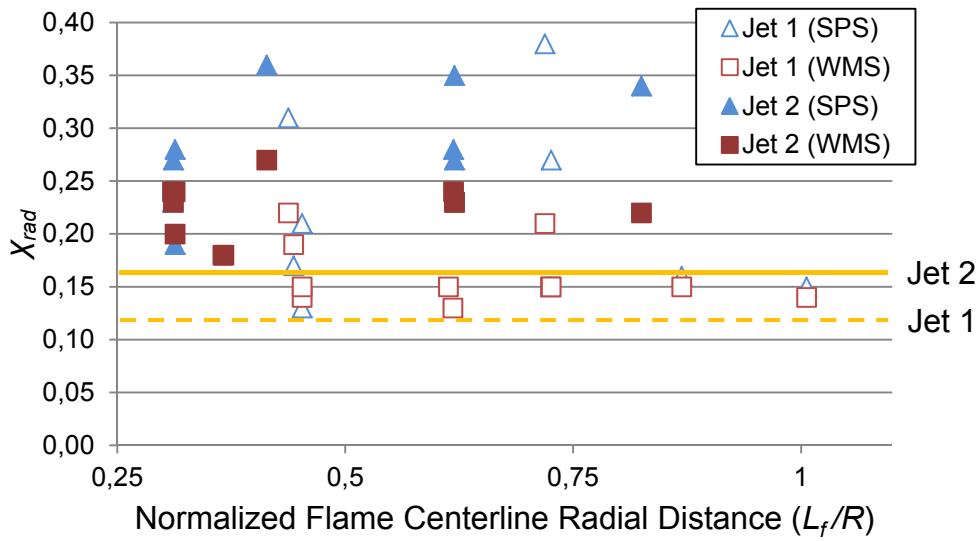

Nonetheless, measured radiant fraction values were still ***~40% higher*** than predictions based on flame residence time correlations.

A surface reflection model with an *assumed* reflectance of 0.5 used to correct for surface irradiance effects:

Jet	d_j [mm]	$\dot{m}$ [kg/s]	L_f [m]	p_0 [barg]	T_0 [K]	RH [%]	T_{amb} [K]	p_{amb} [mbar]	U_{wind} [m/s]	Wind dir [°]
1	20.9	1.0	17.4	59.8	308.7	94.3	280	1022	2.84	68.5
2	52.5	7.4	48.5	62.1	287.8	94.5	280	1011	0.83	34.0

$$C^*_{refl} = \varepsilon \cdot R^2_{ray} \sum_{i=1}^{N} \frac{w_i \cos\beta_{i,obs} \cos\beta_{i,refl}}{D^2_{ray,i}} \frac{A_{clip,i}}{A_{inf,i}} \tau_i$$

$$\Rightarrow \chi = q_{meas} \frac{4\pi}{\dot{m} \cdot \Delta H_c} \frac{1}{\left(\frac{C^*_{inc}}{R^2_{inc}} + \frac{C^*_{refl}}{R^2_{ray}}\right)}$$

WMS point emitters replaced by spheres:

$$r_i = \frac{1}{2} \frac{w_i}{w_{max}} W_f$$

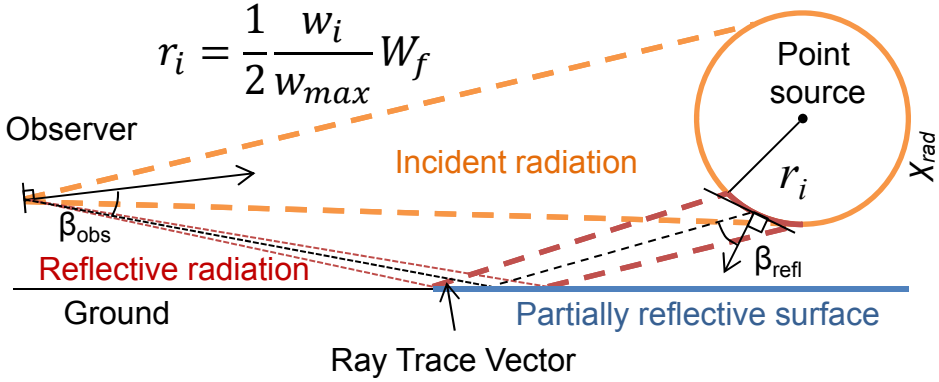

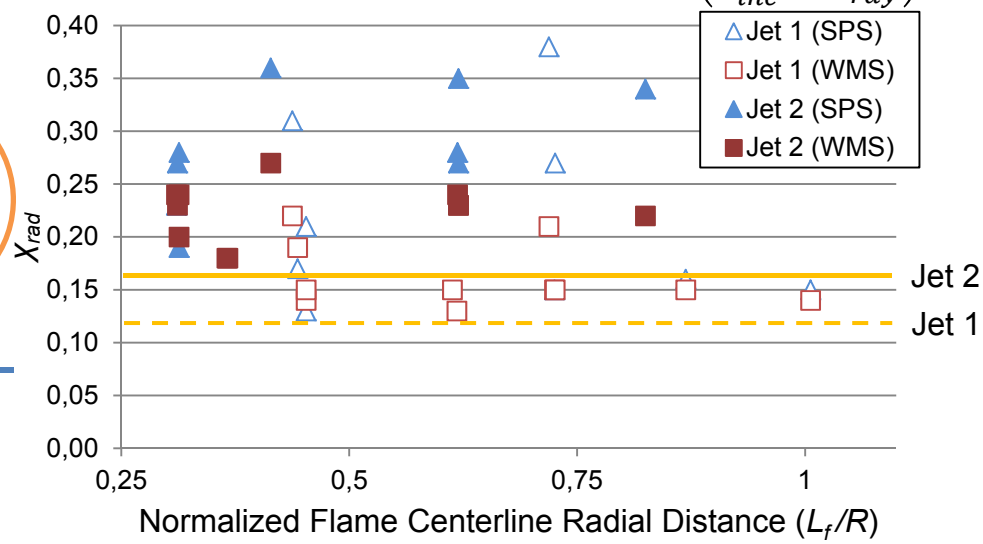

ε:	Surface Reflectance
A_{clip}:	Clipped view area
A_{inf}:	Total view area w/ infinite reflector

A surface reflection model with an *assumed* reflectance of 0.5 used to correct for surface irradiance effects:

Jet	d_j [mm]	$\dot{m}$ [kg/s]	L_f [m]	p_0 [barg]	T_0 [K]	RH [%]	T_{amb} [K]	p_{amb} [mbar]	U_{wind} [m/s]	Wind dir [°]
1	20.9	1.0	17.4	59.8	308.7	94.3	280	1022	2.84	68.5
2	52.5	7.4	48.5	62.1	287.8	94.5	280	1011	0.83	34.0

$$C^*_{refl} = \varepsilon \cdot R^2_{ray} \sum_{i=1}^{N} \frac{w_i \cos\beta_{i,obs} \cos\beta_{i,refl}}{D^2_{ray,i}} \frac{A_{clip,i}}{A_{inf,i}} \tau_i$$

$$\Rightarrow \chi = q_{meas} \frac{4\pi}{\dot{m} \cdot \Delta H_c} \frac{1}{\left(\frac{C^*_{inc}}{R^2_{inc}} + \frac{C^*_{refl}}{R^2_{ray}}\right)}$$

WMS point emitters replaced by spheres:

$$r_i = \frac{1}{2} \frac{w_i}{w_{max}} W_f$$

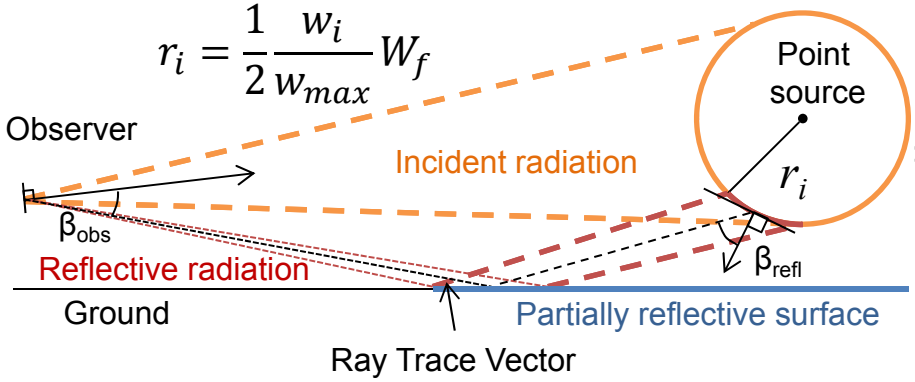

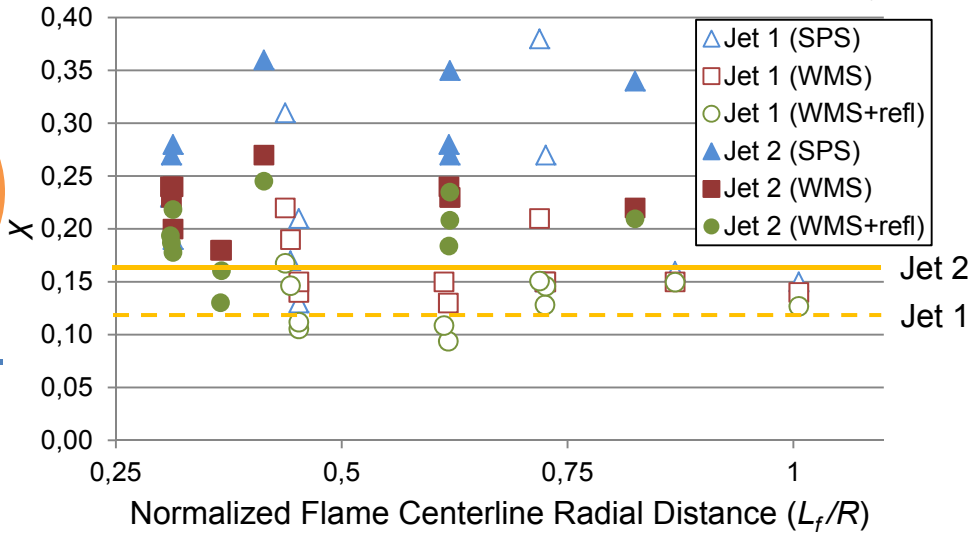

ε:	Surface Reflectance
A_{clip}:	Clipped view area
A_{inf}:	Total view area w/ infinite reflector

Ekoto et al., Proc Int Pipeline Conf, 2012

Measured radiant fractions now within ***~20%*** *of* predictions.

An integral model is needed to handle wind & buoyancy effects

Jet	d_j [mm]	$\dot{m}$ [kg/s]	L_f [m]	p_0 [barg]	T_0 [K]	RH [%]	T_{amb} [K]	p_{amb} [mbar]	U_{wind} [m/s]	Wind dir [°]
1	20.9	1.0	**17.4**	59.8	308.7	94.3	280	1022	2.84	68.5
2	52.5	7.4	**48.5**	62.1	287.8	94.5	280	1011	0.83	34.0

Jet 1 (3/4" diameter)

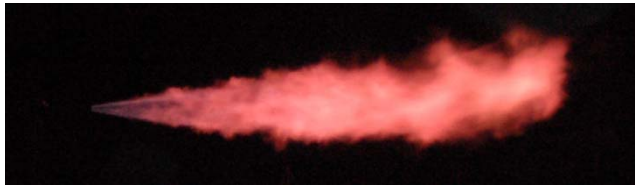

Jet 2 (2" diameter)

Experimental scenario analysis and CFD modeling were used to evaluate indoor refueling hazards.

CFD used to evaluate optimal sensor placement

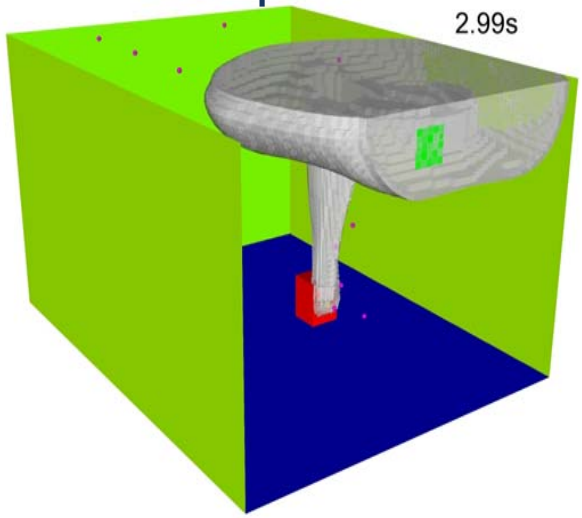

Large-scale experiments

Flame front propagation imaged (3 sec ignition delay)

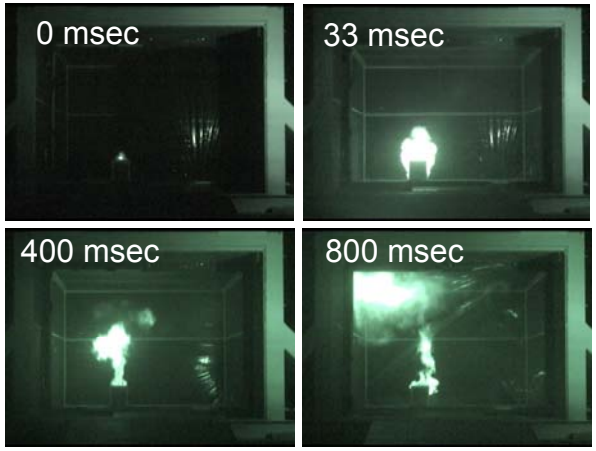

Mitigation measures such as active/passive ventilation and blowout panels examined

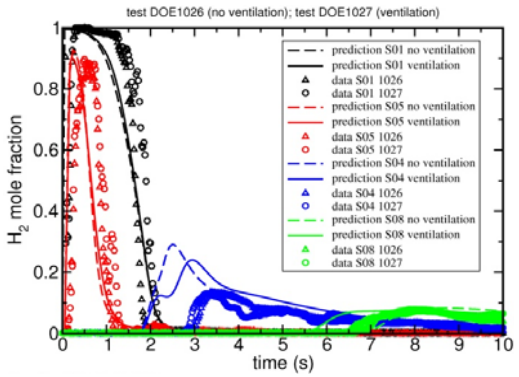

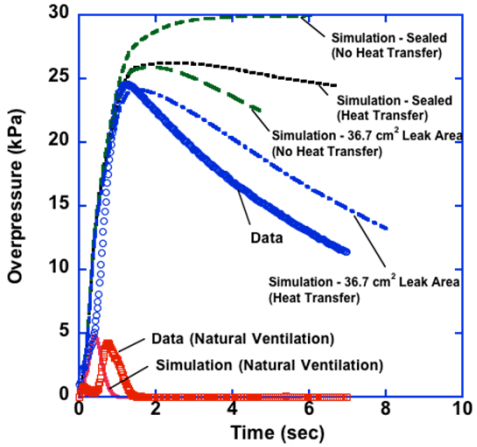

CFD matched the data if wall heat transfer and warehouse leak area corrections were applied.

Summary of Correlation Gaps

General H_2 Release Behavior Gaps:

- Intermittency model needs refinement along with new PDF prediction methods
- PDFs for spatial and temporal integral scales needed
- Data needed to analyze aspect ratios impact for different leak geometries

Ignition Mechanism Gaps:

- Particle laden flow models need to be incorporated w/ existing plume dispersion models
- Charge generation and spark discharge mechanisms need to be investigated.

Flame Light-up Gaps:

- Greater understanding about ignition transition point and/or more data on blowout stability limits is needed.

Hazard Analysis Gaps:

- Integral model needed for large-scale flame radiation modeling
  - Greater consideration of reflective radiation?
- Heterogeneous confined/delayed ignition models are needed
  - Can integral dispersion models be used to form initial conditions?

A significant need exists to consolidate existing models and correlations into some sort of QRA framework

Indoor Non- Public Fast Fill* Dispenser P&ID

Code Compliant

*Note – Fast Fill Doesn't exist in IFC; limits H2 flow to 12 SCFM (0.027kg/min) IFC 2309.3.1.2 (3)

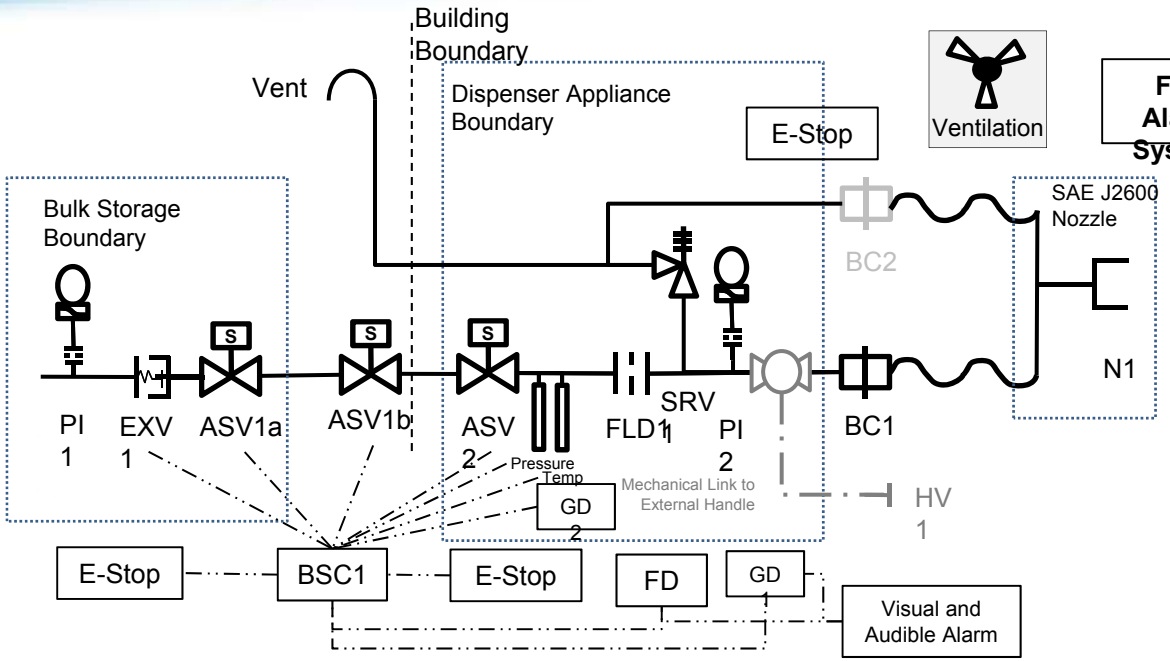

Other Safety Requirements

- Physical Protection – 7.17.7.3
- Ignition Source Control – 7.1.23
- Explosion control- 6.9 when quantity exceeds quantities in Table 6.4.1.1
- Occupancy – 6.1.1.4, 7.1.1.3
- Qualified Operator – **10.3.3.1.1**
- **Minimum Room Volume – Table 10.3.3.2.2.2, 10.3.3.2.2.2 (D) for multiple dispensers**
- **Ceiling height – 10.3.3.2.2.2 (E)**

P&ID Tag	Description	Code/Standard Reference	P&ID Tag	Description	Code/Standard Reference
ASV1a	Auto shutoff (solenoid) valve (Source Valve)	6.20 - Source Valve 7.1.21 - Accessible manual or automatic emergency shutoff valve (HGV 4.4/HGV 4.6 Component Standards)	PI1/PI2	Dispense delivery pressure indicator (6" circular mechanical gauge; 0-10000psig)	10.3.1.5.3 – indication of storage, dispenser discharge pressure 10.3.1.5.2 - 0.055in opening at inlet connection NOTE – a third pressure gauge at compressor discharge is also required (10.3.1.5.3)
ASV1b	Auto shutoff (solenoid) valve (building isolation)	7.1.21.2 …at the point where the system piping enters the building 10.3.1.18.4 – building isolation valve required	SRV1	Safety (Overpressure) relief valve (6000psig)	10.3.1.4.2.3 – overpressure device shall be installed; 10.3.1.4.2.4 – setting shall not exceed 140% of service pressure 10.3.1.10.5 – inspected every 3 years
ASV2	Auto shutoff (solenoid) valve	7.1.21.2 …at the point of use 10.3.3.2.2.7 (A) – Automatic shutoff valve	N1	Nozzle	10.3.1.14.7 – transfer system capable of depressurization to facilitate disconnection 10.3.1.15.1 – SAE J2600 nozzle required
EXV1	Excess Flow Device	7.1.22 Excess flow control – leak detection and emergency shutoff or excess flow control (Component Standard?) 10.3.1.18.3 - excess flow valve requirements	Vent	Vent Pipe and Vent Pipe Termination	6.16 - CGA 5.5, 7.1.17,
FD1	Flame detector	10.3.1.19.1 – gas, flame detected at any point on the equipment 10.3.3.2.2.4 – Fire detection system tied to local visual and audible alarm	Ventilation	Required ventilation for indoor fueling	**10.3.3.2.2.2 – in accordance with 10.3.2.2.1.6** 10.3.2.2.1.6 - required by clause (A) 10.3.2.2.1.6 (D) (1) continuous or activated by h2 detector
GD1, GD2	Gas detector	10.3.1.19.1 – gas, flame detected at any point on the equipment **10.3.3.2.2.7 (E) – GD2 added, inside of the dispenser housing (a class 1 Div 1 area) with similar requirements to 10.3.1.19.1 and with additional requirements: activation shuts down dispenser, visual/audible alarm and functions during maintenance**	**Estop x 3**	Manual Emergency Stops	10.3.1.18.5 – local and remote located manual shutdown **10.3.3.2.2.6 – Emergency shutdown device similar to 10.3.1.18.5 with more specifid locaiton requirments** 10.3.3.2.2.6 (A) – 3rd manual shutdown device on the dispensrer
BC1	Breakaway coupling (dispensing hose)	10.3.1.18.6 – breakaway coupling required – NGV 4.4 compliant, breaking force	H1	Flexible dispensing /vent hose	10.3.1.1 – listed or approved 10.3.1.8 – Hose connections (note – no reference to HGV 4.4 10.3.1.11.2 – Hose assemblies 10.3.3.2.2.2 (H) – limited to 25ft. Protected from abrasion or driven over by vehicle
FLD1	**Flow limiting device**	**10.3.3.2.2.2 (F) max fueling rate 2kg/min**	BC2	Breakaway coupling (vent hose)	Not required
Fire Alarm	**Fire Alarm System**	**10.3.3.2.2.5 – dispensing area local fire alarm system, pull box between 20 and 100 ft of dispenser, at nearest exit from area, pull boxes shutdown dispenser**	**HV1**	**Hand Valve – "quarter turn" manual shutoff**	**10.3.3.2.2.7 (B) - not required when ASV 2 is located immediately upstream and a control arm or ESD closes the valve**
BSC1	Building Safety Circuit (Logic Controller)	10.3.1.11.6 – controller performs 5 sec pressure test prior to fueling 10.3.1.11.7 – repeat integrity check at 3000 psi 10.3.1.18.7 – control circuit requirement for manual reset after emergency stop activation 10.3.3.2.1.9 – manual restart after emergency activation 10.3.3.2.2.2 (C) automatic shutoff control when max fuel quantity per event or vehicle fueled to capacity 10.3.3.2.2.2 (G) – references 10.3.1.11.6 and 10.3.1.11.7 10.3.3.2.2.7 (G) – overpressure and over temperature sensing capabilities (assume that this could be communication with vehicle)			

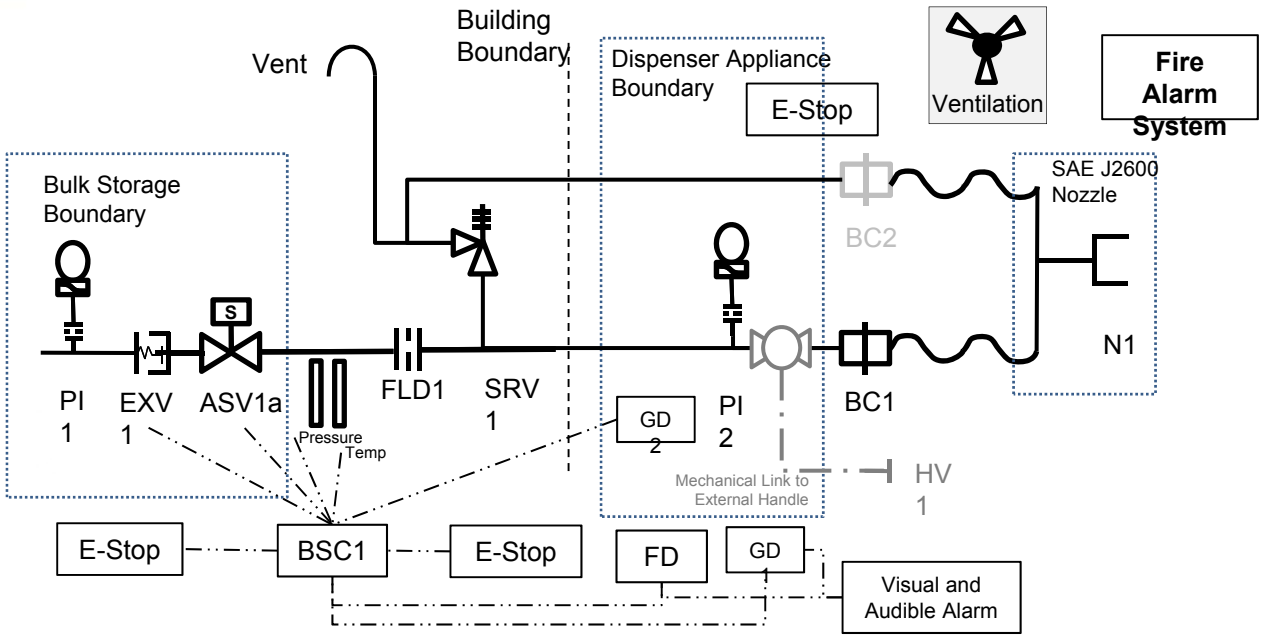

- Controls located outdoors with storage
- Dispenser appliance and number of components indoors reduced
- May not contain gas detector
- Retains required isolation and controls aspects

Indoor Non-Public Fast Fill* Dispenser P&ID

Alt. Case 1

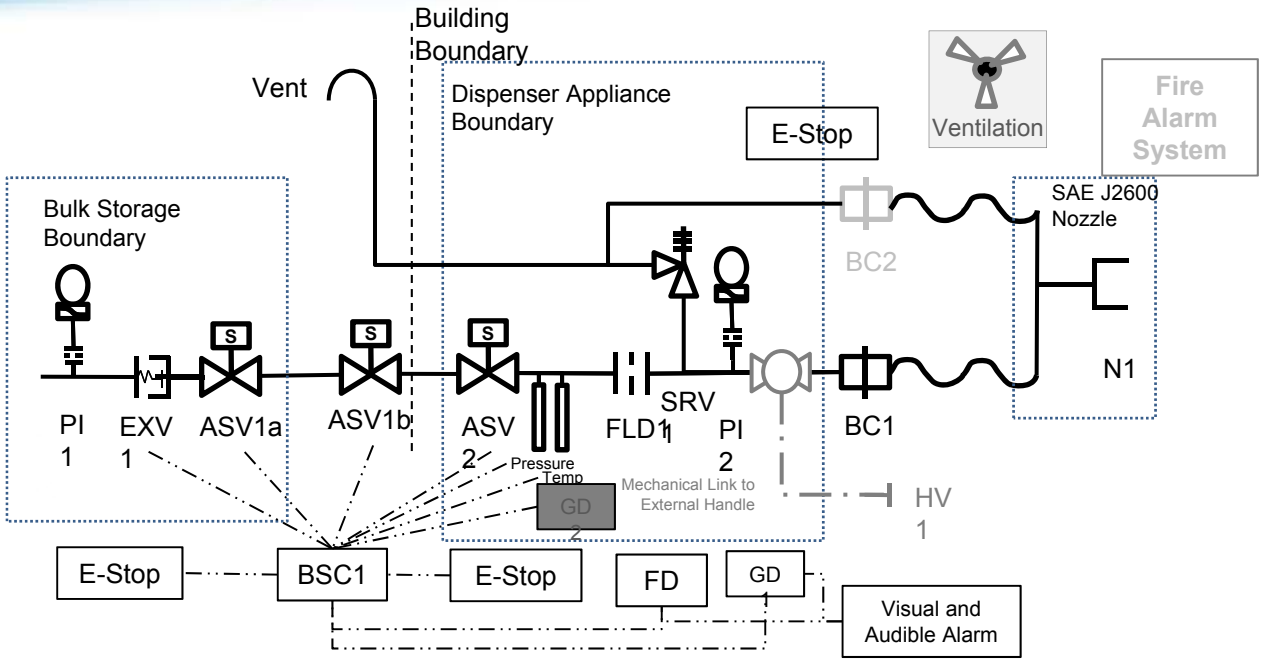

- Remove fire alarm system
- Remove ventilation system
  - e.g., cold storage with limited ventilation & recirculation
- Remove gas detection

Indoor Non-Public Fast Fill* Dispenser P&ID

Alt. Case 2

Without QRA, many of these alternate dispenser layouts would not be possible.

Validated CFD approach used to evaluate full-scale scenarios and inform indoor refueling requirements.

- **Forklift tank and release parameters:**
  35 MPa storage pressure, 0.8 kg H_2, 6.35 mm orifice dia.
- **Warehouse:**
  7.62 m ceiling, 3 room volumes

Analysis performed in support of NFPA 2/55

Flammable H_2 Cloud Development

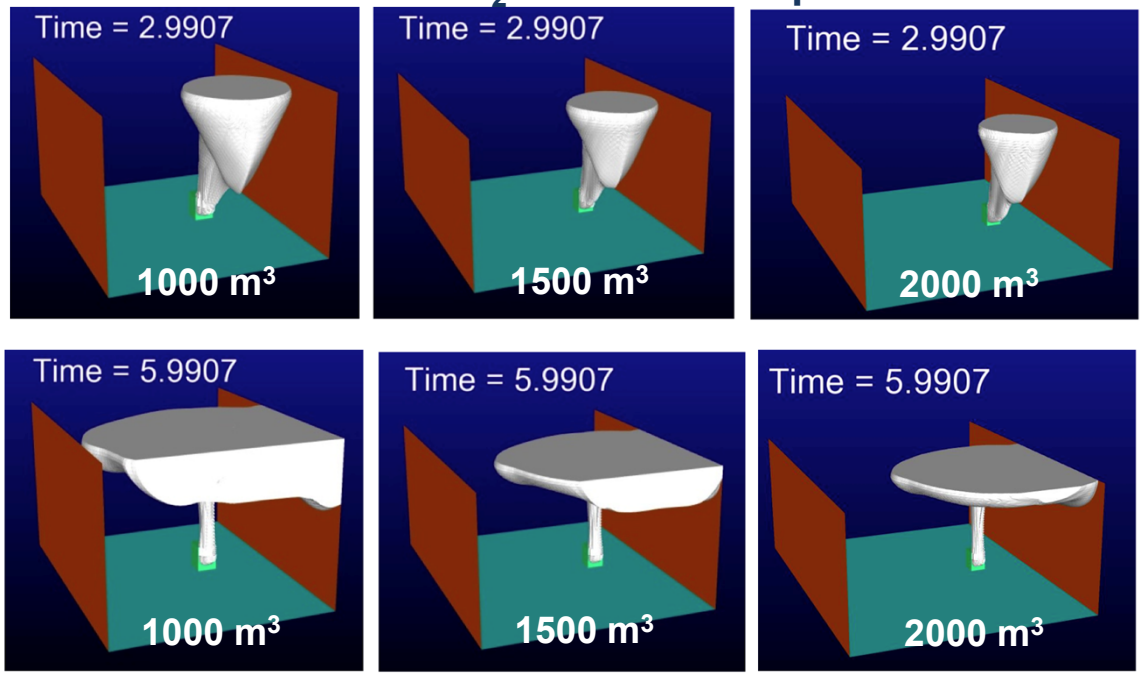

Overpressure vs. Warehouse Volume

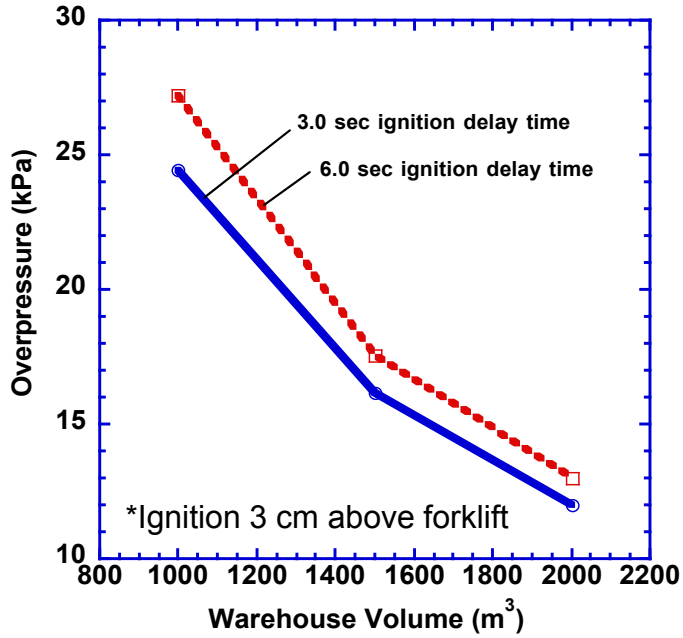

Can dispersion be predicted from integral plume & ceiling layer models?
How do we account for obstacles?
Are reduced order overpressure models using flammable volumes viable?

Scalar field of a momentum driven, turbulent H_2 jet was examined via high-resolution Planar Rayleigh Scatter Imaging (PLRS).

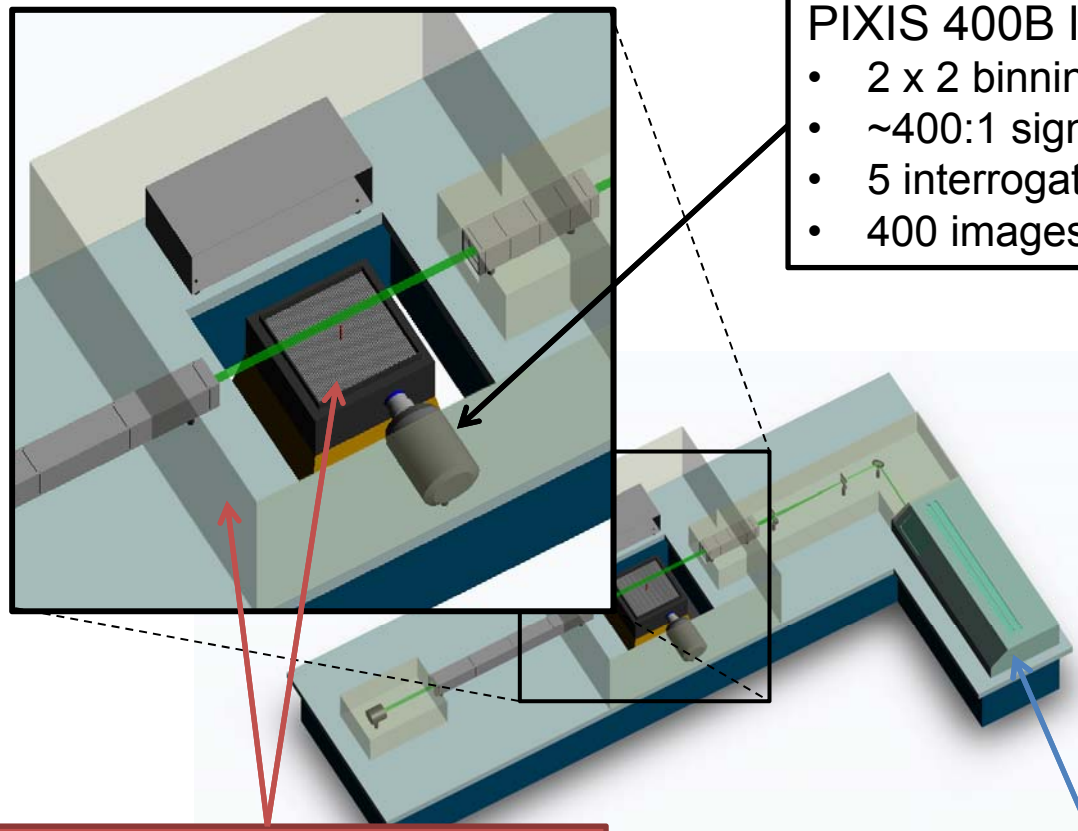

PIXIS 400B low noise CCD Camera
- 2 x 2 binning for 3.94 pix/mm resolution
- ~400:1 signal-to-noise
- 5 interrogation regions (37 x 125 mm^2)
- 400 images per interrogation region

$r_0 = 0.95\ mm$
$L_{pipe} = 250\ mm$
$Q = 100\ lit/min$
$Fr_{den} = 1170$

Air co-flow & barriers to minimize impact of room currents

High power injection seeded Nd:YAG laser (1 J/pulse, 532 nm)

Additional diagnostics include Particle Image Velocimetry (PIV), Laser Doppler Velocimetry (LDV) and OH Laser Induced Fluorescence (LIF).

Self-similarity in the established flow zone requires only centerline values/trajectories to describe plume.

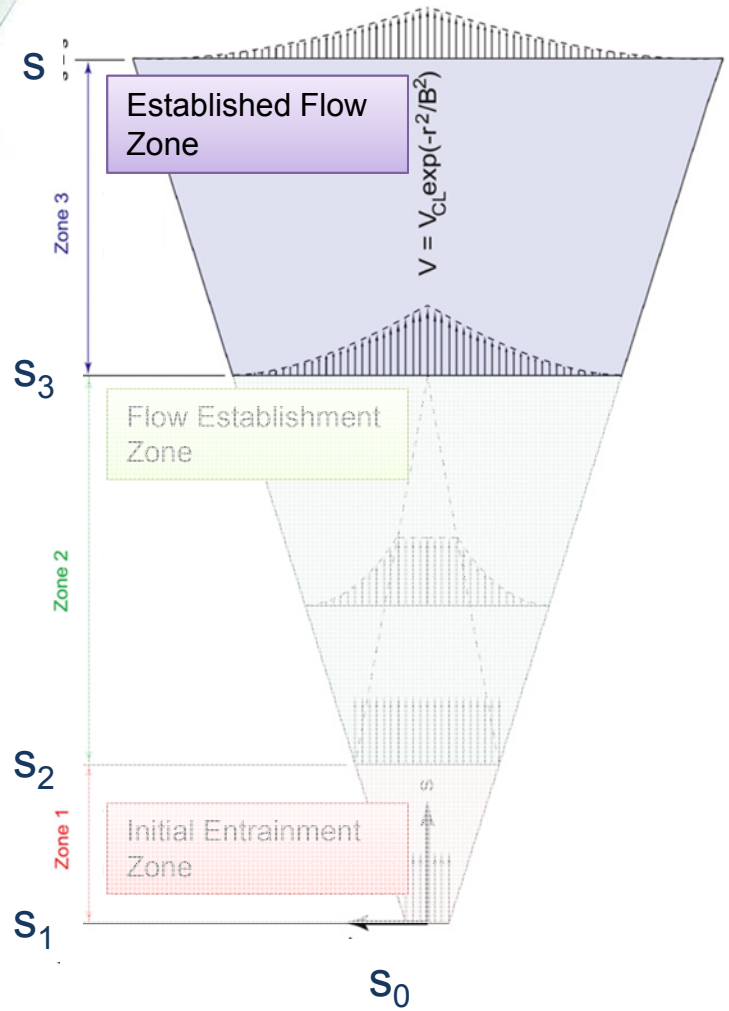

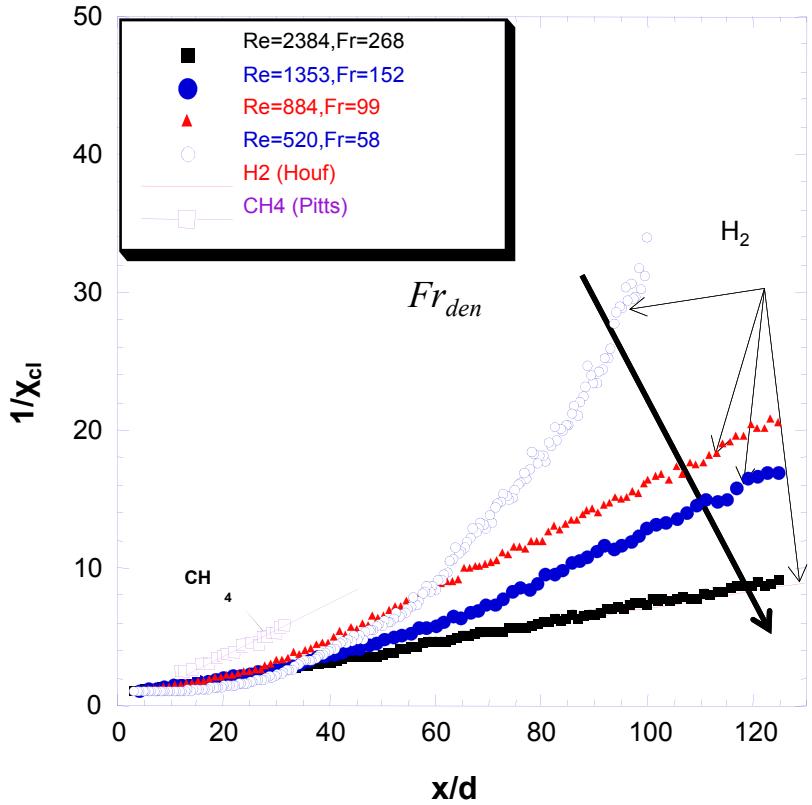

Schefer, Houf, Williams, Int J H_2 Energy, 2008

Zones 1 and 2 generally neglected for small (unchoked) gas leaks from circular orifices.

Raw signal intensity corrections used to create a quantitative concentration image

R:	Raw image
E_B:	Electronic bias
B_G:	Background luminosity
p_F:	Laser power fluctuation
O_R:	Camera/lens optical response
S_B:	Background scatter
S_t:	Laser sheet profile variation
I:	Corrected intensity

$$R = \boxed{p_F \cdot O_R \cdot (I \cdot S_t + S_B)} + E_B + B_G$$

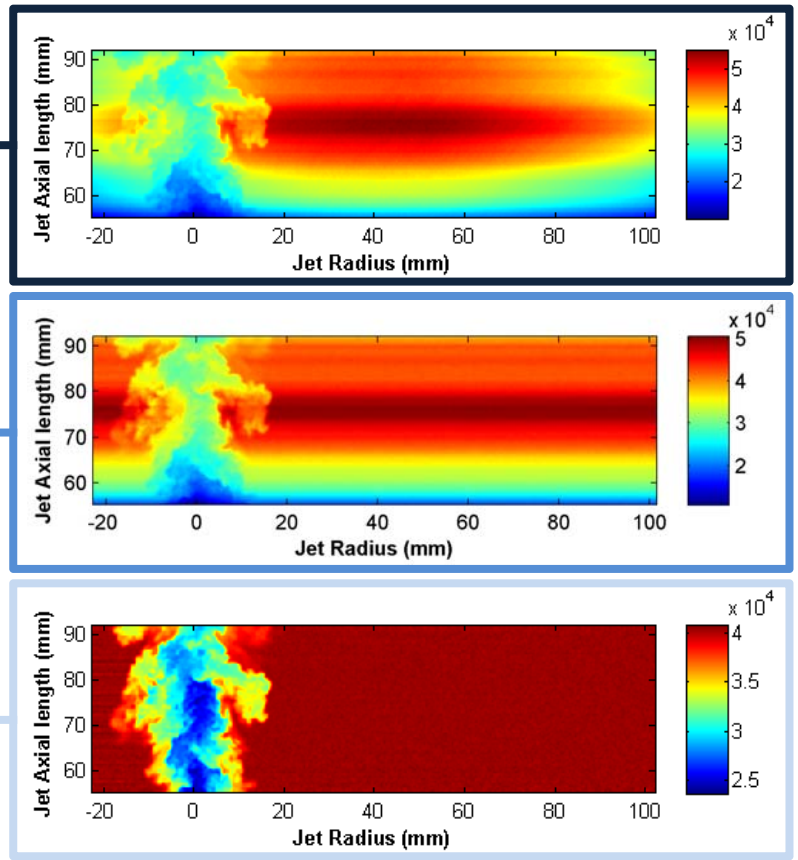

Mole Fraction $(\chi_{H2}) \propto I$

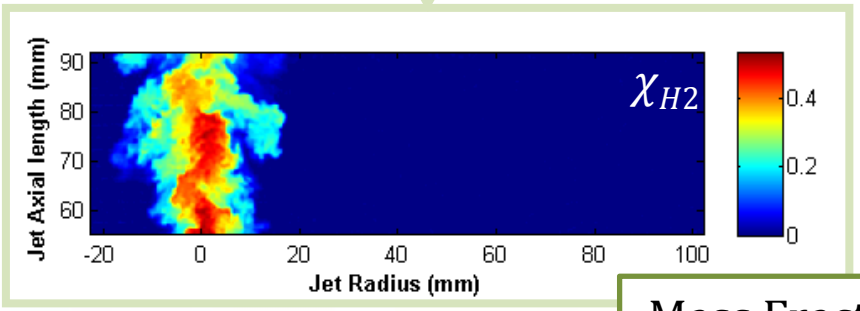

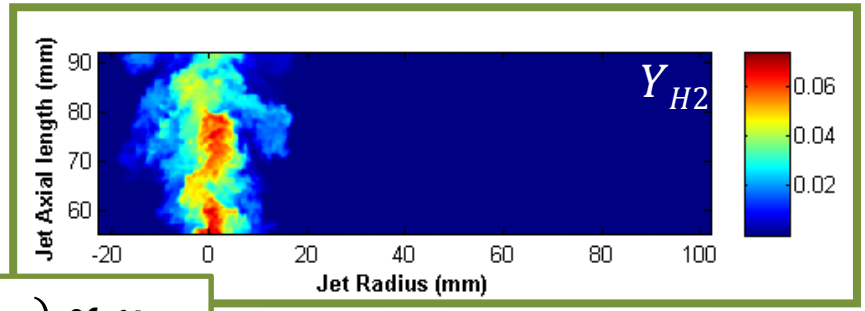

Mass Fraction $(Y_{H2}) \propto \chi_{H2}$

Coordinate critical stakeholders & research to remove technology deployment barriers

Partnerships with industry, labs, academia

Identify R&D needs → *Perform High-Priority R&D* → *Impact Codes and Standards*

Harmonize Internationally

Regulations, Codes and Standards (RCS, GTR)
International Standards (eg. ISO)
International Agreements (IEA, IPHE)

- Metrics for Success
  - Number of codes, standards, regulations impacted
  - Degree of harmonization
  - ***Successful technology deployments***

Incompressible free-jets:

$$\frac{1}{\bar{Y}_{CL}} = K_c \frac{z - z_{0Y}}{r^*} \Longrightarrow r^* = K_c \frac{z - z_{0Y}}{\bar{Y}_{CL}}$$

Where;

$\bar{Y}_{CL}$: centerline mass fraction

$r^* \equiv r_0 \sqrt{\frac{\rho_{jet}}{\rho_{air}}}$: mass weighted effective radius

K_c: centerline decay rate constant

z: axial coordinate

z_{0Y}: mass fraction virtual origin

Seamless reconstruction of mass fraction statistics from stitched together interrogation regions

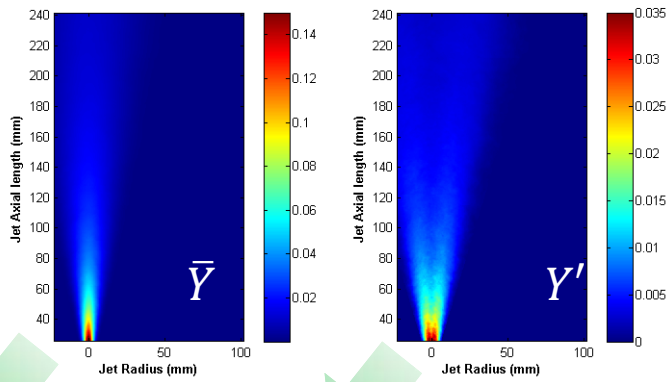

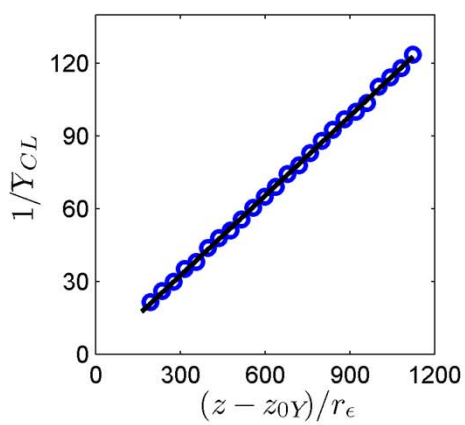

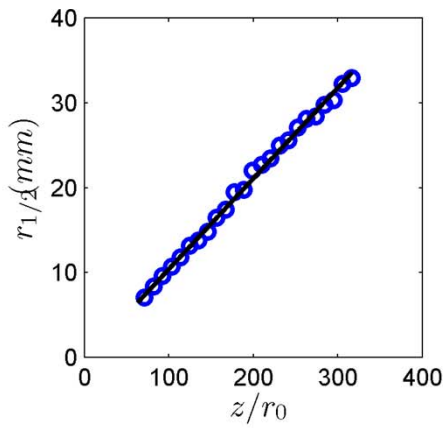

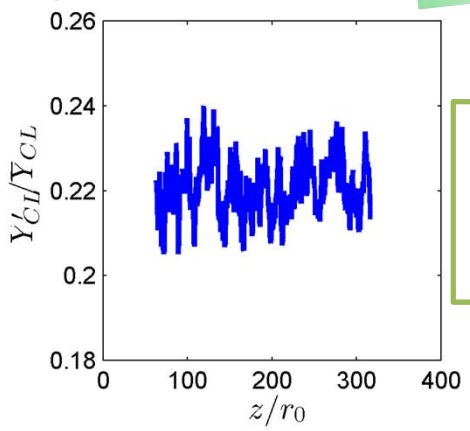

$r_0 = 0.95\ mm$
$L_{pipe} = 250\ mm$
$Q = 100\ lit/min$
$Fr_{den} = 1170$

- Constant centerline decay (= 0.105) and jet spreading rates (0.113)
- Constant unmixedness ($\equiv Y'_{CL}/\bar{Y}_{CL} = 0.22$)

Centerline constants agree very well with literature reported values.

How best can risk management approaches incorporate H_2 behavior models?

Prescriptive

Advantages:

- Straightforward implementation
- Uniform & easily verifiable acceptance criteria
- Works well for clearly defined applications

Disadvantages:

- Unable to weight for harm potential
- Difficult to account for cascade events & complex systems
- Suboptimal resource allocation

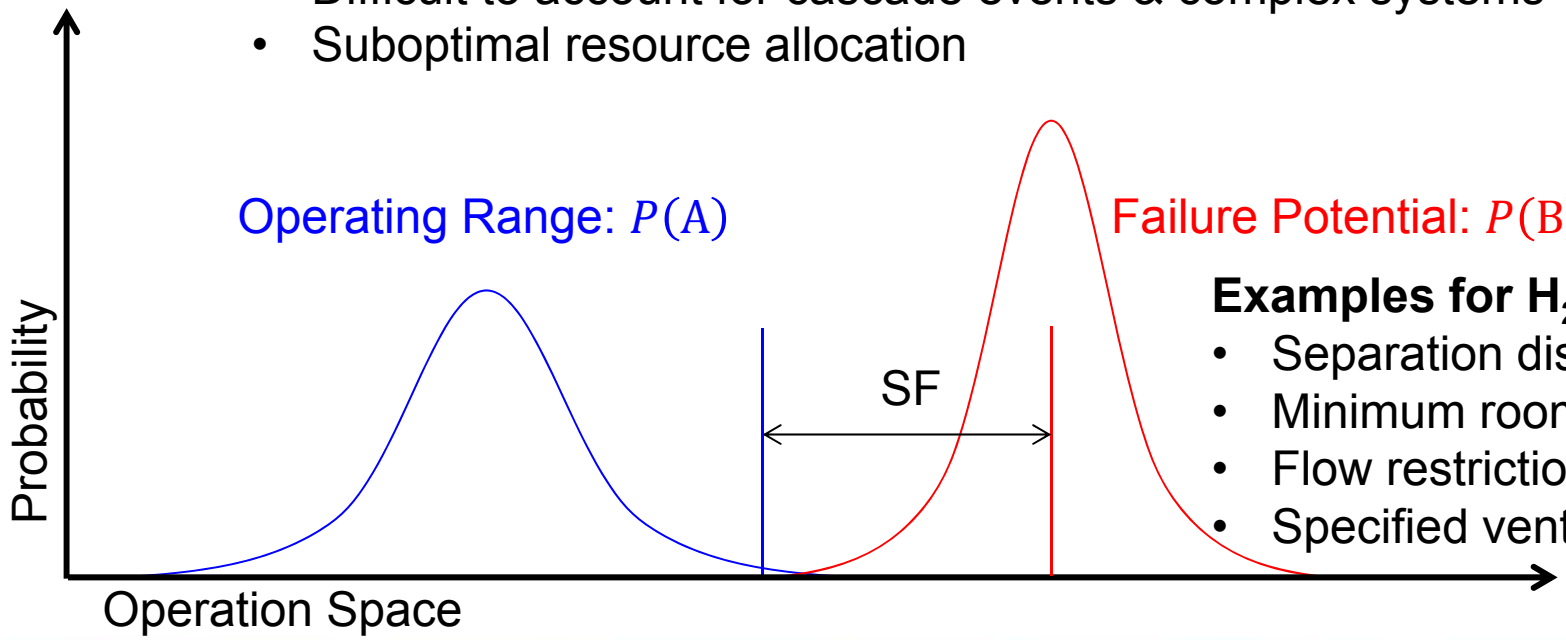

Examples for H_2 SCS:

- Separation distances
- Minimum room volumes
- Flow restriction
- Specified ventilation rates

ESD modeling requires several considerations:

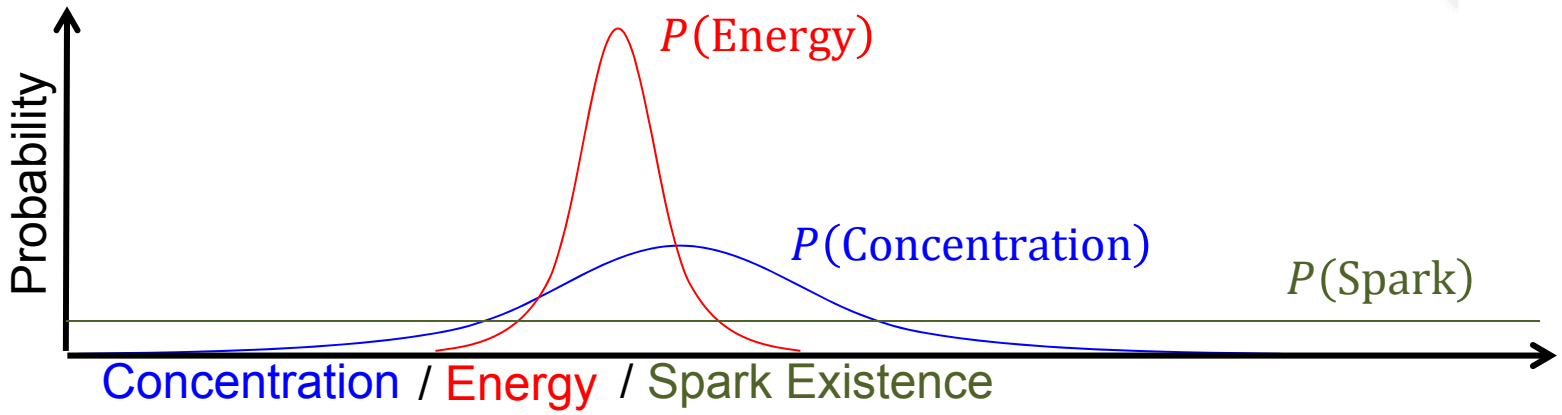

How best can risk management approaches incorporate H_2 behavior models?

QRA

Advantages:

- Risk weighted according to harm potential – resources allocated where needed
- Non-obvious systemic risk can be identified
- Additional risk contributors (i.e., human factors) can be included
- Quantifiable insight into risk mitigation strategies

Disadvantages:

- Complex implementation & certification
- Accurate probabilities require expansive datasets

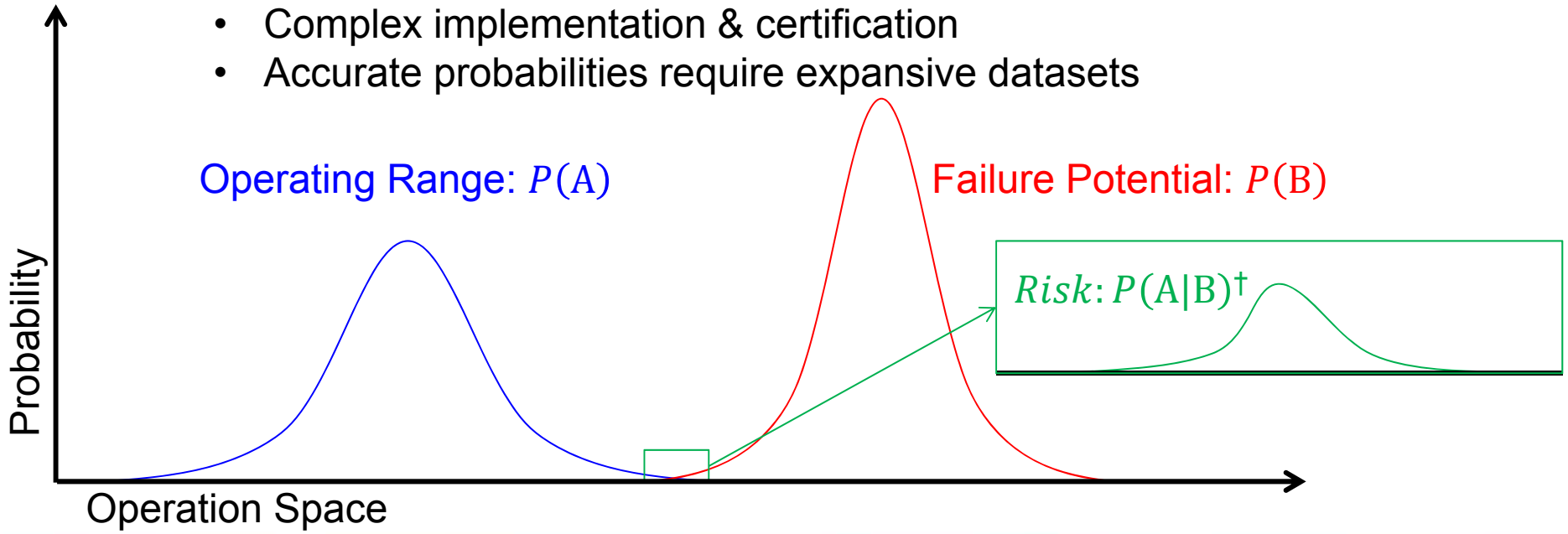

$^{\dagger}P(\mathrm{A}|\mathrm{B})$ conditional probability that event A occurs for a given event B